HHS Public Access

Author manuscript

Connect Tissue Res. Author manuscript; available in PMC 2017 July 01.

Published in final edited form as:

Connect Tissue Res. 2016 July ; 57(4): 319–333. doi:10.1080/03008207.2016.1182996.

Disparate Response of Articular- and Auricular-derived Chondrocytes to Oxygen Tension

Thomas J. Kean[1,2,5,*], **Hisashi Mera**[1,2,4,*], **G. Adam Whitney**[1,2], **Danielle L. MacKay**[1,5], **Amad Awadallah**[2], **Russell J. Fernandes**[3], and **James E. Dennis**[1,2,5]

[1]Matrix Biology Program, Benaroya Research Institute at Virginia Mason, Seattle, WA, USA

[2]Department of Orthopedics, Case Western Reserve University, Cleveland, OH, USA

[3]Department of Orthopaedics and Sports Medicine, University of Washington, Seattle, WA, USA

[4]Department of Health and Sports Sciences, Mukogawa Women's University, Hyogo, Japan

[5]Department of Orthopedic Surgery, Baylor College of Medicine, Houston, TX, USA

Abstract

Purpose/Aim—To determine the effect of reduced (5%) oxygen tension on chondrogenesis of auricular-derived chondrocytes. Currently, many cell and tissue culture experiments are performed at 20% oxygen with 5% carbon dioxide. Few cells in the body are subjected to this supra-physiological oxygen tension. Chondrocytes and their mesenchymal progenitors are widely reported to have greater chondrogenic expression when cultured at low, more physiological, oxygen tension (1–7%). Although generally accepted, there is still some controversy, and different culture methods, species, and outcome metrics cloud the field. These results are, however, articular chondrocyte biased and have not been reported for auricular-derived chondrocytes.

Materials and Methods—Auricular and articular chondrocytes were isolated from skeletally mature New Zealand White rabbits, expanded in culture and differentiated in high density cultures with serum free chondrogenic media. Cartilage tissue derived from aggregate cultures or from the tissue engineered sheets were assessed for biomechanical, glycosaminoglycan, collagen, collagen cross-links, and lysyl oxidase activity and expression.

Results—Our studies show increased proliferation rates for both auricular and articular chondrocytes at low (5%) O_2 versus standard (20%) O_2. In our scaffold free chondrogenic cultures, low O_2 was found to increase articular chondrocyte accumulation of glycosaminoglycan, but not cross-linked type II collagen, or total collagen. Conversely, auricular chondrocytes accumulated less glycosaminoglycan, cross-linked type II collagen and total collagen under low oxygen tension.

Corresponding author. Thomas J. Kean, Department of Orthopedic Surgery, Baylor College of Medicine, 1 Baylor Plaza, ABBR730, Houston, TX, USA, tjkean@bcm.edu, Tel: 713-986-6025 Fax: 713-798-5443.

*These authors contributed equally to the manuscript

Conflict of Interest

The authors declare that they have no conflicts of interest with the contents of this article.

Conclusions—This study highlights the dramatic difference in response to low O_2 of chondrocytes isolated from different anatomical sites. Low O_2 is beneficial for articular-derived chondrogenesis but detrimental for auricular-derived chondrogenesis.

Keywords

Chondrogenesis; Collagen cross-linking; Articular chondrocytes; Auricular chondrocytes; Oxygen tension; Cartilage tissue engineering

Introduction

The field of tissue engineering is starting to realize some of its promise with tissue engineered bladders surviving in patients for more than 11 years (1). Articular cartilage tissue engineering has, however, remained a challenge. Significant clinical success has been seen with autologous chondrocyte implantation (ACI) and matrix-induced autologous chondrocyte implantation (MACI) (2,3). However, histological analyses showed that more than 50% of patients had fibrous cartilage repair (3,4).

Current clinical approaches involve the expansion and implantation of articular chondrocytes harvested from a low-load bearing area of the joint (5). At least two issues may disadvantage the use of this donor site, 1) joint damage may have compromised the cells harvested from this site, 2) the cartilage is hypocellular, so cells isolated from small amounts of tissue must undergo significant expansion to give adequate numbers for ACI, MACI or tissue engineering. Chondrocytes undergo significant de-differentiation with increased population doublings, resulting in a cell that poorly re-differentiates into cartilage like tissue (6). Cartilage tissue has significant similarity across sources, i.e. articular, epiglottal, nasal, meniscal and auricular (7). This similarity raises the possibility of using non-articular sources for joint repair (8). Cartilage produced by chondrocytes of all five sources is generally avascular, hypocellular, and matrix-rich. The extracellular matrix has high glycosaminoglycan (9) and collagen content. However, while ostensibly similar, there are biochemical and mechanical differences between the sources and cartilage characteristic of hyaline, elastic or fibro-cartilage (7). An advantage to auricular cartilage is that it is easily harvested with minimal morbidity (10). Our group has had significant success in producing scaffold-free tissue engineered auricular cartilage sheets with favorable mechanical characteristics that could enable total joint resurfacing, tracheal and auricular reconstruction (11–15). Xu et al. (2004) observed that non-expanded porcine auricular chondrocytes embedded in fibrin gel and implanted subcutaneously in nude mice gave greater biomechanical and GAG values than articular or intercostal cartilage constructs (16). Clinical auricular reconstruction with subcutaneously implanted culture expanded auricular chondrocytes has also shown impressive results (17). *In vitro* tissue engineering of scaffold-free cartilage sheets for tracheal replacement found that the auricular source gave the greatest accumulation of GAG and collagen and had superior mechanical properties (13,14).

Oxygen tension has long been known to impact the development of tissues, with chondrogenesis being promoted by reduced oxygen tension (18). The *in vivo* partial pressure of oxygen in articular cartilage has been estimated to be ~1% at the growth plate and up to

~10% at the articulating surface (19). In nasal cartilage, it is reported to be 1–3% *in vivo* (20). We are not aware of any reported measurement or estimate for auricular cartilage. More physiological oxygen tensions have been broadly investigated in articular chondrocytes and mesenchymal stem cells for chondrogenesis (Table 1). In general, reduced oxygen tension enhances articular chondrogenesis, primarily in terms of gene expression and GAG accumulation (Table 1). The effect of oxygen tension is less clear with respect to collagen content, and studies investigating mechanical characteristics are rare. Current dogma is that low oxygen tension stimulates chondrogenesis (21–23). However, we are not aware of any investigations into the effects of low oxygen tension on auricular chondrocytes. Also, given the somewhat variable effects of oxygen tension reported (Table 1), the effect of low oxygen tension on articular chondrogenesis, especially in terms of mechanical strength and collagen cross-linking, deserved further analysis.

Based on the preponderance of evidence from previous studies on articular chondrocytes and their progenitor, mesenchymal stem cells, it was hypothesized that low (5%) oxygen tension would enhance chondrogenesis in terms of the accumulation of GAG and collagen, collagen cross-linking and mechanical strength for both articular and auricular chondrocytes.

Materials and Methods

Chondrocyte harvest, isolation, and expansion

Native ear (auricular) and humeral head (articular) cartilage tissues were harvested from adult, 12–16 month-old, male New Zealand White rabbits in accordance with the guidelines of the ACUC of Case Western Reserve University and the University of Washington. Chondrocytes were isolated from these tissues as previously described (12,13), plated at 5.7 × 10^3 cells/cm^2 in T-175 cell culture flasks (431080; Corning, Lowell, MA) and grown in expansion medium (Dulbecco's modified Eagle's medium [DMEM] with 1g/L glucose (Invitrogen, Grand Island, NY) supplemented with 10% fetal bovine serum [FBS, Invitrogen; lot# 281497]) under standard conditions (humidified atmosphere, 37°C, 20% O_2, 5% CO_2). Medium was changed every 3 to 4 days. Chondrocytes were split from each prep at the end of primary (P0) and first passage (P1) into two equal groups and further expanded at 20% or 5% O_2 using a CO_2/N_2 incubator (MCO-18AIC; Sanyo, Tokyo, Japan). Medium changes, passaging, and the preparation for aggregate and engineered cartilage, were performed under standard O_2 conditions as previously described (12).

Aggregate culture and harvest

Aggregates were made from TC-expanded cells as described previously (6). Briefly, 250,000 cells were dispensed into several wells of a sterilized (autoclaved) polypropylene v-shaped bottom 96-well plate (Phenix, Hayward, CA), centrifuged at 590 RCF for 10 min, and placed in chondrogenic medium (serum-free DMEM with 4.5g/L glucose, containing 1% sodium pyruvate, and 1% penicillin/streptomycin [all from Invitrogen], 1% ITS-premix [BD Bioscience], 100 nM dexamethasone [Sigma-Aldrich], and 37.5 μg/mL L-ascorbate-2-phosphate [Wako chemicals]. The aggregates were cultured under the same oxygen condition as that used in expansion, and medium was changed every other day. At 21 days, the aggregates were collected and processed for combined GAG and DNA analysis (3

aggregates from each group), for combined collagen and collagen cross-links analysis (3 aggregates from each group), for lysyl oxidase (LOX) activity assay (3 aggregates from each group), for LOX gene expression analysis (3 aggregates from each group, stored in RNA Later® [Qiagen] at −80°C), and fixed in neutral buffered formalin for histology (1 aggregate from each group). Wet weights of all aggregates were taken after blotting excess media using filter paper.

Scaffold-free tissue-engineered cartilage sheet culture

Chondrocytes were applied to a custom double-diffusion biochamber with porous (10 μm pore diameter) polyester membrane (PET 1009030; Sterlitech, Kent, WA), which had been precoated with 5 μg/ml fibronectin (BD Bioscience, San Jose, CA), as previously described (11), at a density of 3.13×10^6 cells/cm^2. The cells were cultured under the same O_2 condition as in expansion with bioreactor medium (serum-free DMEM with 4.5 g/L glucose (Invitrogen, Grand Island, NY), containing 1% ITS-premix (BD Bioscience, San Jose, CA), 100 nM dexamethasone (Sigma-Aldrich), 37.5 μg/mL L-ascorbate-2-phosphate (Wako chemicals, Osaka, Japan), and 1% sodium pyruvate, 1% non-essential amino acid, 1% glutamax, and 1% Penicillin/Streptomycin (all from Invitrogen, Grand Island, NY)). The medium was changed every other day. After 3 weeks, cartilage sheets were removed from the biochamber and allowed to free float until 6.5 weeks. Punches (5 mm in diameter) were taken for the mechanical testing from each sheet. Combined GAG/DNA analysis was made in triplicate (3 mm diameter punches), as was collagen/collagen cross-link analysis. Histology was performed on a single neutral buffered formalin fixed 3 mm punch from each sheet. The sheets were made in duplicate from 4 donors.

Assessment of population doublings

After tissue culture expansion under low (5%) or standard (20%) oxygen tension, at the end of P1 and P2 stages, the number of viable cells under both conditions were counted by trypan blue exclusion with a hemocytometer to determine cell doublings per day during expansion, as previously described (24), i.e., Population doubling rate (PD/day) = ($\log_2$ (#cells at the end of passage/#cell seeded))/days in culture.

Biomechanical analysis for scaffold-free engineered cartilage

Mechanical properties of the engineered cartilage sheets, Poisson’s ratio and aggregate modulus, were determined by indentation testing, as previously described (15). Samples were adhered to a stainless steel platen using cyanoacrylate. This maintains the no-slip and no-fluid-flow boundary conditions at the cartilage-substrate interface, which are used as constants in data processing to obtain mechanical properties. During testing, samples were bathed in phosphate-buffered saline. A cylindrical porous stainless steel tip with a diameter of 1.07 mm was used to apply tare and test loads to samples, and displacement was measured using a linear variable transducer. After displacement reached equilibrium under the tare load, the test load was applied and displacement over time was recorded. A 1g test load was chosen to limit the engineered cartilage compressive strain to ~20%. Aggregate modulus and shear modulus were determined as parameters of biphasic stress-strain equations fit to test load-displacement data as described (25,26).

Biochemical analyses

GAG, hydroxyproline (HDP) and DNA analyses—Samples of engineered cartilage were analyzed for their biochemical content. Initially GAG/DNA were assessed as previously described (27), and, later, a combined GAG/HDP/DNA assay was developed. In both cases, samples were digested in papain solution (200 μl of 25 μg/mL papain, 2 mM cysteine, 50 mM sodium phosphate, and 2 mM EDTA adjusted to pH 6.5 [all from Sigma-Aldrich]) at 65° for 3 h. At this point, for the combined GAG/HDP/DNA assay, half of the sample was taken into a new tube and processed as described below. For the GAG/DNA assay portion, papain digested solutions were incubated with 2 volumes of 0.1 M sodium hydroxide (NaOH) for 30 min at room temperature. Two volumes of neutralizing solution was added (5 M sodium chloride and 100 mM disodium phosphate dibasic, pH 7.2; brought to a final concentration of 0.1 M hydrochloric acid). Neutralized samples and a chondroitin sulfate (Seikagaku Chemicals) standard curve were mixed with Safranin-O solution (0.05 % in 50 mM sodium acetate) in duplicate on a dot blot apparatus with a 0.45 μm nitrocellulose membrane (162-015; Bio-Rad, Hercules, CA). Safranin-O was extracted from the nitrocellulose membrane by incubation of the punched dots with 1 ml of 10 % cetylpyridinium chloride (Alpha Aesar), 37 °C for 20 min. This was pipetted into a clear 96-well polystyrene microplate in triplicate, measured by absorbance (536 nm; OPTImax tunable microplate reader with Softmax pro control software ver. 4.3; Molecular Devices LLC., Sunnyvale, CA), and the GAG concentration calculated from the standard curve. For DNA content, aliquots of the neutralized papain digested samples and a calf thymus DNA standard curve were transferred to a black 96-well plate in triplicate, mixed with Hoechst dye (33258; Sigma-Aldrich, 1 mg/ml stock diluted 1/1500 in 0.2 M pH 8 phosphate buffer), and read using a fluorescent plate reader (Ex 365 nm, Em 460 nm; Fusion with Instrument control application ver. 4.02; PerkinElmer Inc., Boston, MA). HDP was assessed on the portion aliquoted prior to alkalization and neutralization using the method previously described (15). Briefly, the samples were hydrolyzed overnight (1 ml 6 M HCl; 110 °C in boil-proof polypropylene tubes), cooled and tubes uncapped then dried at 65–70 °C. Samples and hydroxyproline standards were resuspended in ddH_2O and mixed with 1 volume of 0.15 M copper sulfate, 1 volume of NaOH and incubated at 40 °C for 5 min. To this, 1 volume of hydrogen peroxide (6%) was added and incubated for 10 min at 40 °C. After cooling, 4 volumes of sulfuric acid (6 M) and 2 volumes of Ehrlich's reagent (5% p-dimethyl-amino-benzaldehyde [Sigma] in 60 % n-propanol, 26 % perchloric acid, 14 % water) were added and incubated at 70 °C for 16 min before cooling and transferred, in triplicate, to a 96-well plate. Absorbance was read at 492 nm and hydroxyproline content calculated from the standard curve. Collagen content was estimated from the hydroxyproline concentration with the conversion factor of 7.6 (28).

Histology—The tissues for histology were fixed with 10% formalin, dehydrated through a graded series of alcohol washes, and embedded in paraffin. Paraffin sections were stained with safranin-O for GAG detection, and Fast Green was used as a counterstain. For immunohistochemistry, slides were deparaffinized, hydrated, and antigen retrieval performed by incubation with pronase (1 mg/ml in PBS containing 5 mM calcium chloride; Sigma-Aldrich) for 10 min at room temperature. Sections were then incubated with PBS/BSA for 10 min at room temperature, then overnight at 4 °C with primary antibody (mouse anti-type

II collagen – DSHB II-II6B3, 1/500 in PBS/BSA, mouse anti-typeX collagen – kind gift of Gary Gibson (Henry Ford Hospital, Detroit, MI) - 1/500 in PBS/BSA, mouse anti-elastin – millipore MAB2503, 1/200 in PBS/BSA). After 3 washes, secondary antibody (biotin conjugated goat anti-mouse; Cappel 1/200 in PBS/BSA) was added and sections incubated for 1 h at room temperature. After 3 washes, sections were incubated with streptavidin-HRP (Gibco, 1/200 in PBS/BSA) at room temperature for 30 min. Slides were washed 3 times and detection performed using Vector VIP peroxidase (SK-4600; Vector Labs). Slides were then counterstained with Fast Green (0.0125% in 25 % ethanol, 0.875 % glacial acetic acid) 10 s, then dehydrated and mounted with Permount (Fisher Scientific).

Collagen cross-link analysis—Samples were dried, weighed and acid hydrolyzed in 6M HCl, 110 °C for 24h. Hydroxylysyl pyridinoline (HP) and Lysyl pyridinoline (LP) cross-linking residues were resolved and quantified by C-18 reverse phase HPLC with fluorescence detection (excitation 297 nm, emission 396 nm) and total collagen content was determined as described (29).

Collagen heteropolymer analysis—Samples were dried using a kimwipe and weighed. The heteropolymeric collagen network formed in the samples was depolymerized in equal volumes of 0.5 M acetic acid containing 100 μg/ml pepsin for 18 h at 4 °C. Extracted collagen was analyzed by SDS-PAGE and the separated collagen chains visualized by Coomassie blue staining. Pepsin-extracted type II collagen from rabbit articular cartilage was use as a control. The separated collagen chains were also blotted onto PVDF membrane and probed with mAb 1C10 to identify α1(II) chains. After stripping, the western blot was sequentially probed with mAb 10F2 and pAb 5890 to identify collagen chains cross-linked to the C-telopeptide of α1(II) and to the N-telopeptide of α1(XI) chains. As we have described before, this validates if a heteropolymer of type II and type XI collagen had formed (30).

LOX gene expression analysis—Total RNA was extracted from aggregate samples. Aggregates were thawed in RNA later solution, tissue was transferred to an RNase free custom made stainless steel 24-well pulverizer on dry ice, and pulverized. 300 μL of solution D (4 M guanidium thiocyanate, 25 mM sodium citrate, pH 7.0, 0.5% sarcosyl with DEPC-H_2O, 0.2M sodium acetate (pH 2.0), 7.2% 2-mercaptoethanol [Fisher Biotech, Fair Lawn, NJ]) was added to the crushed sample. This solution would freeze in the well; then, the pulverizer was transferred to a water bath (65 °C, 5–7 min). After all the solutions were thawed, the lysate/homogenates were transferred and further homogenized with QIAshredder (Qiagen), then mixed with phenol/ chloroform/ isoamyl alcohol solution, and total RNA purified following conventional phenol/chloroform extraction methods. RNA purity and concentration was confirmed by NanoDrop analysis (260 nm/280 nm ratio). Reverse transcription reaction was performed with an equal amount of RNA from both hypoxic and standard samples according to the manufacturer's protocol (Random hexamers; Applied Biosystems [ABI], Foster city, CA). The real-time PCR to detect LOX and 18S gene expression was performed with SYBR green (Maxima SYBR Green qPCR Master Mix; Fermentas/ Thermo Scientific, Eugene, OR) using a 7500 HT real-time PCR system (ABI). Samples were initially denatured at 95 °C for 2 min and then subjected to 40 repeated

cycles of: denature at 95 °C for 15 s, annealing at 55 °C for 45 s, elongation at 72 °C for 30 s. Expression levels of LOX were normalized to 18S rRNA levels for each sample. The primer sets were designed as follows: LOX-forward; GACCCGTACAACCCCTACAAG; LOX-reverse; AGCACCCTGTGGTCATAGTCTC; 18S forward; CTCAACACGGGAAACCTCAC; 18S reverse; TTATCGGAATTAACCAGACAAATCG. The human 18S primers (31) were tested *in silico* against the rabbit RNA sequence (NR_033238.1 using Primer-BLAST) and for primer dimers using Eurofins Oligo Analysis Tool; 100% sequence coverage and acceptable self-complementarity were found. Experimentally, 18S primers were 99.8% efficient for a 5-log dilution of rabbit cDNA with a single melting point of 81.89 °C. LOX primers were designed and tested using Primer-Blast against the predicted rabbit sequence (XM_002710146.1) and acceptable self-complementarity was also found. Experimentally, LOX primers were 98.7% efficient for a 5-log dilution of rabbit cDNA with a single melting point of 86.57 °C.

LOX activity assay—The aggregates for LOX activity assay were homogenized in 4M urea in 0.02M borate buffer (pH 8.2) at 4°C and were centrifuged at 15,000 RCF for 30 min at 4°C, and the protein concentration of the supernatants measured using the bicinchoninic acid assay according to the manufacturer's instructions (Promega). Aliquots of 10 μg protein extract were analyzed immediately for the assay with or without LOX-specific inhibitor β-propionitrile (BAPN; Sigma-Aldrich). The sample solution was added to the final reaction mixture (50 mM sodium borate [pH 8.2], 1.2 M urea, 50 μM N-acetyl -3,7-dihydroxyphenoxazine (Amplex Red; Molecular Probes-Invitrogen), 0.1 U/ml horseradish peroxidase (HRP; Sigma-Aldrich), and 10 mM 1,5-diaminopentane substrate (Cadaverine dihydrochloride; Sigma-Aldrich) in the presence or absence of 500 μM BAPN (Alfa-Aesar, Ward hill, MA), as previously described (32,33). LOX acts on Cadaverine (pseudosubstrate) and produces H_2O_2, and the HRP-catalyzed oxidation of *N*-acetyl-3,7-dihydroxyphenoxazine by H_2O_2 produces fluorescent resorufin. The fluorescence was read every 20 min for 2 hours at 37°C using a multimode plate reader (Fusion with Instrument control application ver. 4.02; PerkinElmer Inc., Boston, MA). LOX activity was calculated from the slope which was corrected for non-specific signal by subtracting BAPN-containing values from BAPN-free values, and normalized to the DNA content.

Data analysis and statistics

Each data point represents the mean for replicates within that experiment (replicates ≥ 2); data are then summarized as mean ± standard deviation for each group. An experiment (n) is defined by rabbit donor and passage; numbers of experiments are indicated below graphs and all n are ≥ 4. Experiments were performed at passage 1 and 2. Differences between groups and conditions were assessed by one-way ANOVA, with Sidak's correction for multiple tests. For tests between the two oxygen tensions with the same passage/donor, a ratio paired t-test was used. Statistical analyses were performed using Graph Pad Prism 6 (Graph Pad Software, Inc.). Values of $p < 0.05$ were considered to indicate statistically significant differences; * $p < 0.05$, ** $p < 0.01$, ***$p < 0.0001$.

Results

Proliferation rate

Chondrocytes expanded at a faster rate when cultured at 5% O_2 than at 20% O_2 for both auricular and articular chondrocytes. Although the magnitude of this difference was small, its effect is exponential. The proliferation rate of auricular chondrocytes at 5% O_2 was 0.51 ± 0.13 PD/day, 3% higher than cells from the same rabbit at 20% O_2 (0.50 ± 0.13 PD/day; Fig. 1). The proliferation rate of articular chondrocytes at 5% O_2 was 0.28 ± 0.08 PD/day, 16% higher than cells from the same rabbit cultured at 20% O_2 (0.24 ± 0.07 PD/day; Fig. 1). Auricular chondrocytes grew significantly more quickly than articular chondrocytes at either oxygen tension ($p < 0.0001$).

Engineered cartilage: Aggregate wet weight, GAG, and collagen content

Wet weights of auricular-derived aggregates showed no significant differences between the two oxygen tensions, while articular-derived aggregates at 5% O_2 were significantly heavier than those at 20% O_2 (Fig. 2). The GAG content of auricular aggregates cultured in 5% O_2 was significantly decreased compared to those at 20% O_2 (Fig. 3), while articular-derived aggregates cultured at 5% O_2 tended to have greater GAG content then those cultured at 20% O_2 (Fig. 3). GAG content for auricular chondrocytes cultured at 20% O_2 was significantly higher than all other conditions ($p < 0.0001$). Collagen content of auricular aggregates was also significantly decreased through culture at 5% O_2 vs 20% O_2, with no apparent effect on articular chondrocytes (Fig. 4).

Lysyl oxidase expression, activity and effect on collagen cross-links

Lysyl oxidase expression was unchanged in auricular chondrocyte aggregates grown at 5% O_2 vs. 20% O_2, while articular chondrocyte aggregates showed an increased lysyl oxidase expression at 5% O_2 vs. 20% O_2 (Fig. 5A). Although the gene expression of lysyl oxidase in auricular aggregates was unchanged by oxygen tension, its activity was significantly decreased in aggregates cultured at 5% O_2 vs. 20% O_2 (Fig. 5B). There was no apparent difference in the activity of lysyl oxidase in the articular chondrocytes at different oxygen tensions (Fig. 5B). This difference in lysyl oxidase activity is reflected in the density of the collagen cross-links found within the tissue, with auricular chondrocytes grown at 5% O_2 having significantly less collagen cross-links than those grown at 20% O_2 (Fig. 6). As expected from the LOX activity, there was no significant effect of oxygen tension on the collagen cross-links in articular chondrocyte matrix.

Histology

Safranin-O staining showed results compatible with total GAG/DNA analysis (Fig. 2), where 5% O_2 decreased the accumulation of GAG in the matrix of auricular aggregates but increased its accumulation in articular aggregates (Fig. 7A–D). Collagen type II is strongly expressed in auricular aggregates (Fig. 7E–F), but a reduced intensity at 5% O_2 is apparent at higher magnification (Fig. 8E–F). Collagen type II accumulation in the articular aggregates is greater in 5% O_2 conditions than 20% O_2, and appears more evenly distributed in the matrix (Fig. 7G–H). Type X collagen, commonly found in native auricular tissue, is

downregulated in 5% O_2 vs. 20% O_2 and is more intracellular (Fig. 7I–J); higher magnification images are shown in Fig. 8I–J. Collagen type X staining is weak in articular chondrocytes and is predominantly cell associated. There is a semblance of more matrix accumulation at 5% O_2 vs. 20% O_2 (Fig. 7K–L). Higher magnification images confirmed this cell associated staining (Fig. 8K–L). Elastin, natively expressed by auricular chondrocytes, is weakly expressed by auricular chondrocytes across all conditions with only 20% O_2 micrographs showing any appreciable accumulation (Fig. 7M–P and Fig. 8M–P).

Mechanical strength

In order to investigate the effect of low oxygen tension on mechanical strength, scaffold-free tissue engineered sheets were produced for mechanical testing. Auricular chondrocytes failed to produce testable sheets at low oxygen tension (3 of 3 donors), but articular sheets showed a significant increase in stiffness through culture at 5% oxygen tension (Fig. 9). Auricular chondrocyte sheets produced at 20% oxygen tension had aggregate moduli of 0.229 MPa ± 0.04 and native bovine articular cartilage had an aggregate modulus of 0.371 MPa ± 0.07.

Collagen heteropolymer analysis

Figure 10A shows that the major pepsin resistant Coomassie blue-stained band in both the auricular and articular chondrocyte cultures migrated identically to the α1(II) chain of type II collagen in the control. β1(II) chains (dimers of α1(II) chains) were also observed in all lanes. Two faintly stained bands migrating slightly slower than that of the α1(II) chains, best visualized in lane 6, were identified by mass spectrometry as the α1(XI) and α2(XI) chains of type XI collagen (data not shown) and also described in (34). No other major pepsin resistant bands were stained, indicating that type II collagen and type XI collagen were the major collagens synthesized by the cultured chondrocytes and the cartilage collagen phenotype was maintained even after 6.5 weeks in culture. The α1(I) and α2(I) chains of type I collagen were not detected in either tissue engineered cartilage. Although immunohistochemistry detected type X collagen in standard (20% O_2) auricular cartilage cultures (Figs. 7 and 8), no pepsin resistant Coomassie blue stained type X collagen chains were observed in the expected 55–60 kDa range (data not shown). The western blot shown in Fig. 10B confirms that the Coomassie blue stained bands were indeed α1(II) chains of type II collagen. Using mAb 1C10, which specifically recognizes type II collagen chains (35), intense staining of both the α1(II) and β1(II) chains were observed. Since equivalent loads were electrophoresed in all the lanes, densitometry of the Western blot revealed moderately higher levels of type II collagen (α1(II) + β1(II)) reactivity in the 20% O_2 auricular culture when compared to 5% O_2. However for the articular cartilage cultures, there were comparable levels at both oxygen tensions. This is consistent with the results in Fig. 4. In the articular cartilage lanes, mAb 1C10 also recognized low molecular weight fragments of α1(II) chains, and occasionally recognized higher molecular weight fragments of β1(II) chains, which have been identified as pepsin over-cleavage products of type II collagen (29).

Having quantitated that both hydroxylysyl pyridinoline and lysyl pyridinolines cross-link residues in these cultures (Fig. 6), we identified precise domains of collagen chains that are

cross-linked using a recently refined western blot method (36). To show that type II and type XI collagen molecules in these cultures were stabilized by these cross-links, we used the pAb 5890 (34,36). As seen in Fig. 10C, this antibody recognized the α1(II) chains and the β1(II) chains of type II collagen. As we have shown before (34,36), this means that the N-telopeptide of the α1(XI) chain to which this antibody was raised was cross-linked to the helical lysine (L930) residue in a fraction of α1(II) chains of type II collagen molecules and thus a hetero-polymer of type II and type XI collagens had formed in the cultures. Under standard culture (20% O_2) conditions, auricular chondrocytes seem to have higher levels of this cross-link when compared to hypoxic conditions. This was not evident for articular chondrocyte cultures, where equivalent levels were observed. A faint reactivity of the α1(XI) chain was observed in standard (20% O_2) articular cartilage culture that probably indicated an N-telopeptide of one α1(XI) chain to α1(XI) helical lysine cross-link of another chain had formed and a homo-polymer of type XI collagen had also formed in these cultures.

Finally, as seen in Fig. 10D, Western blotting using mAb 10F2 (30,36) again recognized the α1(II) and β1(II) chains in all the cultures. This is evidence that the C-telopeptide of the α1(II) chain specifically recognized by this antibody was cross-linked to the helical lysine (L930) residues in the α1(II) collagen chains and, thus, type II to type II collagen cross-links had also formed in these cultures (30,36). Under standard (20% O_2) conditions both auricular and articular chondrocyte cultures seem to have a higher level of these cross-links when compared to hypoxic conditions (compare intensities in Figs. 10B, 10C and 10D). As explained in (36), it must be reiterated that pepsin-extracted α1(II) collagen is devoid of telopeptides unless they are cross-linked to the lysine residues in the helical regions of α1(II) chains. The data confirms that a heteropolymer of collagen type II and collagen type XI is formed in tissue engineered cartilage sheets from both auricular and articular chondrocyte sources, and a mature collagenous network of cross-linked fibrils had formed.

Discussion

The importance of the control of oxygen tension in cell and tissue culture is often overlooked. This report clearly shows a dramatic difference between the response of rabbit articular and auricular chondrocytes to low (5%) vs. standard (20%) oxygen tension during expansion and re-differentiation. While multiple studies have investigated the effect of oxygen tension on articular chondrocytes (Table 1), the effect of oxygen tension on *in vitro* auricular chondrogenesis is described here for the first time. We have also further clarified the data on articular chondrocyte biology at low (5%), more physiological, oxygen tension.

Articular Chondrogenesis

In scaffold-free culture systems, using both the cell aggregate and sheet approaches to fabricate cartilage, articular chondrocyte constructs had increased GAG accumulation at 5% O_2. Oxygen tension of 5% did not have a positive effect on total collagen accumulation. This is in agreement with several studies (Table 1) including our own on human articular chondrocytes (6). Gel electrophoresis and western blotting also showed that 5% O_2 did not increase cross-linked type II collagen accumulation in the matrix (Fig. 10). In spite of this,

mechanical stiffness of the engineered cartilage significantly increased at low O_2 (Fig. 9). This indicates that it may not be the absolute amount of collagen or proteoglycan in the matrix influencing these properties but rather the proportion of collagen to proteoglycan that accumulates in the matrix. Alternatively, it is due to the increase in GAG content while collagen content is maintained above a threshold level.

Lysyl oxidase is an important enzyme in the stabilization of the collagen network in cartilage, necessary in forming aldehyde-derived pyridinoline cross-links between collagen fibers (37). Low oxygen tension increased lysyl oxidase mRNA expression, but this did not translate into increased lysyl oxidase activity. The reason for this is not clear, but Makris et al.,(38)have proposed that lysyl oxidase activity could be reduced due to a lack of copper ions in defined culture medium. Nevertheless, articular cartilage-like pyridinoline cross-links were detected in the type II collagen under both oxygen conditions.

Auricular chondrogenesis

The dramatically different response of auricular chondrocytes to low oxygen tension was somewhat surprising. It is clear that auricular chondrocytes exhibit significantly lower GAG and collagen deposition when cultured at low oxygen tension in comparison to traditional cultures at standard (20%) oxygen tension (Figs. 3 and 4). Although gene expression of lysyl oxidase was comparatively high for auricular chondrocytes over articular chondrocytes in both conditions, lysyl oxidase activity was significantly decreased by low oxygen tension. The diminished lysyl oxidase activity correlated with a reduction in pyridinoline cross-links in collagen at low O_2 tension. Whether the reduction in collagen cross-linking was responsible for the decreased accumulation of GAG and collagen within the construct is not known, but it has been proposed by Asanbaeva et al. (2008) that these molecules are released into the culture media (39). Lysyl oxidase has also been shown to cross-link elastin (40), but as elastin was weakly expressed in chondrogenic culture, this is thought to have had minimal effect on the outcomes reported. Weak elastin staining was also reported by others in auricular chondrocyte constructs (41). The effect of oxygen tension on auricular chondrocytes may be species specific; as rabbits are known to thermo-regulate through their ears (42), the cartilage therein would be expected to experience greater oxygen tension at times. The difference in response could be due to the fact that auricular cartilage is of neural crest origin while articular cartilage is derived from the mesoderm (43,44). Interestingly, Malda et al., (2004) established that human nasal chondrocytes, which are also derived from the neural crest, are more chondrogenic when cultured under reduced oxygen conditions (45). What is evident from our study is that, under *in vitro* tissue culture conditions, oxygen tension has significant and differing effects on chondrogenesis from two anatomic regions in the same animal.

In a rabbit model (46) and minipig model (47) of articular repair, Lohan et al. found inferior healing in constructs seeded with auricular chondrocytes. Our study could explain their observations. We show that auricular chondrocyte constructs produced at low oxygen tension, as would be expected in the joint, were poorly chondrogenic. Auricular chondrocytes implanted subcutaneously both in humans (17) and in a xenogenic nude mouse model (16,48) seemed to perform well, although neither Xu et al. (16) nor Yokoyama et al.

(48) tested the partial pressure of oxygen in their models. The partial pressure of subcutaneous oxygen is 40–50 mmHg which equates to 5.2–6.5% O_2 (49,50). Besides this, there are additional factors benefiting the delivery of oxygen to the *in vivo* construct, such as haemoglobin's oxygen release profile (51) and fluid flow mass transfer effects (52), and these make comparisons of chondrogenesis with our static culture conditions difficult to interpret. Auricular chondrocytes also produce glycosaminoglycan and collagen rich constructs *in vivo* (16,48). Xu et al. presented data indicating that auricular-derived chondrocyte constructs outperformed costal and articular chondrocytes in terms of both GAG and mechanical strength but not in collagen content. This is corroborated by our data, with higher GAG, collagen, collagen cross-linking and collagen type II staining in auricular-derived constructs at standard O_2 when compared to articular chondrocytes. However, auricular chondrocyte sheets cultured in hypoxic conditions failed to produce mechanically testable sheets. It is likely that other differentiation culture systems will be similarly affected by oxygen tension and, like growth factor and media supplements, this is an essential component of *in vitro* developmental mimicry.

Whilst both articular and auricular cartilage are avascular themselves, the perichondium surrounding auricular cartilage is rich in blood vessels in both humans and rabbits (53). However, auricular cartilage does not benefit from mechanical perfusion mechanisms, creating fluid flow into and out of the tissue, thereby improving nutrient and waste exchange. Future studies investigating the *in vivo* partial pressure of oxygen in rabbit and human auricular cartilage would be of great use in defining an optimal *in vitro* culture system. In addition, studies using flow vs. compression to increase the mass transfer effect would investigate the potential differences in articular vs. auricular response to these different mechanisms of nutrition.

In conclusion, oxygen tension has significant effects on chondrocyte differentiation. Specifically, low oxygen tension is beneficial for articular chondrocyte accumulation of GAG, but its effects on collagen accumulation and cross-linking are negligible. Even so, mechanical properties were significantly improved. Scaffold free constructs formed from auricular chondrocytes at low oxygen tension, however, are deficient in GAG and collagen and are structurally insubstantial and mechanically unsound.

Acknowledgments

Funding was provided through NIH grants AR053622 and DE015322 to J.E.D. and AR057025 to R.J.F.

Abbreviations used

ACI	autologous chondrocyte implantation
BAPN	β-propionitrile
DEPC	diethylpyrocarbonate
GAG	glycosaminoglycan
HDP	hydroxyproline

ITS	insulin, transferrin, selenium
LOX	lysyl oxidase
MACI	matrix assisted autologous chondrocyte implantation

References

1. Atala A. Regenerative bladder augmentation using autologous tissue-when will we get there? J Urol. 2014; 191:1204–1205. [PubMed: 24568815]
2. Peterson L, Vasiliadis HS, Brittberg M, Lindahl A. Autologous chondrocyte implantation: a long-term follow-up. Am J Sports Med. 2010; 38:1117–1124. [PubMed: 20181804]
3. Gobbi A, Chaurasia S, Karnatzikos G, Nakamura N. Matrix-Induced Autologous Chondrocyte Implantation versus Multipotent Stem Cells for the Treatment of Large Patellofemoral Chondral Lesions: A Nonrandomized Prospective Trial. Cartilage. 2015; 6:82–97. [PubMed: 26069711]
4. Gikas PD, Bayliss L, Bentley G, Briggs TW. An overview of autologous chondrocyte implantation. J Bone Joint Surg Br. 2009; 91:997–1006. [PubMed: 19651824]
5. Brittberg M, Lindahl A, Nilsson A, Ohlsson C, Isaksson O, Peterson L. Treatment of deep cartilage defects in the knee with autologous chondrocyte transplantation. N Engl J Med. 1994; 331:889–895. [PubMed: 8078550]
6. Kean TJ, Dennis JE. Synoviocyte Derived-Extracellular Matrix Enhances Human Articular Chondrocyte Proliferation and Maintains Re-Differentiation Capacity at Both Low and Atmospheric Oxygen Tensions. PLoS One. 2015; 10:e0129961. [PubMed: 26075742]
7. Naumann A, Dennis JE, Awadallah A, Carrino DA, Mansour JM, Kastenbauer E, Caplan AI. Immunochemical and mechanical characterization of cartilage subtypes in rabbit. J Histochem Cytochem. 2002; 50:1049–1058. [PubMed: 12133908]
8. Kuhne M, John T, El-Sayed K, Marzahn U, Aue A, Kohl B, Stoelzel K, Ertel W, Blottner D, Haisch A, Schulze-Tanzil G. Characterization of auricular chondrocytes and auricular/articular chondrocyte co-cultures in terms of an application in articular cartilage repair. Int J Mol Med. 2010; 25:701–708. [PubMed: 20372812]
9. Sgaglione NA, Chen E, Bert JM, Amendola A, Bugbee WD. Current strategies for nonsurgical, arthroscopic, and minimally invasive surgical treatment of knee cartilage pathology. Instr Course Lect. 2010; 59:157–180. [PubMed: 20415378]
10. El Sayed K, Haisch A, John T, Marzahn U, Lohan A, Muller RD, Kohl B, Ertel W, Stoelzel K, Schulze-Tanzil G. Heterotopic autologous chondrocyte transplantation--a realistic approach to support articular cartilage repair? Tissue Eng Part B Rev. 2010; 16:603–616. [PubMed: 20825360]
11. Gilpin DA, Weidenbecher MS, Dennis JE. Scaffold-free tissue-engineered cartilage implants for laryngotracheal reconstruction. Laryngoscope. 2010; 120:612–617. [PubMed: 20058322]
12. Henderson JH, Ginley NM, Caplan AI, Niyibizi C, Dennis JE. Low oxygen tension during incubation periods of chondrocyte expansion is sufficient to enhance postexpansion chondrogenesis. Tissue Eng Part A. 2010; 16:1585–1593. [PubMed: 19958052]
13. Henderson JH, Welter JF, Mansour JM, Niyibizi C, Caplan AI, Dennis JE. Cartilage tissue engineering for laryngotracheal reconstruction: comparison of chondrocytes from three anatomic locations in the rabbit. Tissue Eng. 2007; 13:843–853. [PubMed: 17394383]
14. Weidenbecher M, Tucker HM, Awadallah A, Dennis JE. Fabrication of a neotrachea using engineered cartilage. Laryngoscope. 2008; 118:593–598. [PubMed: 18197138]
15. Whitney GA, Mera H, Weidenbecher M, Awadallah A, Mansour JM, Dennis JE. Methods for producing scaffold-free engineered cartilage sheets from auricular and articular chondrocyte cell sources and attachment to porous tantalum. Biores Open Access. 2012; 1:157–165. [PubMed: 23514898]
16. Xu JW, Zaporojan V, Peretti GM, Roses RE, Morse KB, Roy AK, Mesa JM, Randolph MA, Bonassar LJ, Yaremchuk MJ. Injectable tissue-engineered cartilage with different chondrocyte sources. Plast Reconstr Surg. 2004; 113:1361–1371. [PubMed: 15060348]

17. Yanaga H, Imai K, Koga M, Yanaga K. Cell-engineered human elastic chondrocytes regenerate natural scaffold in vitro and neocartilage with neoperichondrium in the human body post-transplantation. Tissue Eng Part A. 2012; 18:2020–2029. [PubMed: 22563650]
18. Bassett CA, Herrmann I. Influence of oxygen concentration and mechanical factors on differentiation of connective tissues in vitro. Nature. 1961; 190:460–461. [PubMed: 13687643]
19. Grimshaw MJ, Mason RM. Bovine articular chondrocyte function in vitro depends upon oxygen tension. Osteoarthritis Cartilage. 2000; 8:386–392. [PubMed: 10966846]
20. Reuther MS, Briggs KK, Schumacher BL, Masuda K, Sah RL, Watson D. In vivo oxygen tension in human septal cartilage increases with age. Laryngoscope. 2012; 122:2407–2410. [PubMed: 22740061]
21. Archer CW, Francis-West P. The chondrocyte. Int J Biochem Cell Biol. 2003; 35:401–404. [PubMed: 12565700]
22. Gibson JS, Milner PI, White R, Fairfax TP, Wilkins RJ. Oxygen and reactive oxygen species in articular cartilage: modulators of ionic homeostasis. Pflugers Arch. 2008; 455:563–573. [PubMed: 17849146]
23. Malda J, Martens DE, Tramper J, van Blitterswijk CA, Riesle J. Cartilage tissue engineering: controversy in the effect of oxygen. Crit Rev Biotechnol. 2003; 23:175–194. [PubMed: 14743989]
24. Solchaga LA, Penick K, Goldberg VM, Caplan AI, Welter JF. Fibroblast growth factor-2 enhances proliferation and delays loss of chondrogenic potential in human adult bone-marrow-derived mesenchymal stem cells. Tissue Eng Part A. 2010; 16:1009–1019. [PubMed: 19842915]
25. Mak AF, Lai WM, Mow VC. Biphasic indentation of articular cartilage--I. Theoretical analysis. J Biomech. 1987; 20:703–714. [PubMed: 3654668]
26. Mow VC, Gibbs MC, Lai WM, Zhu WB, Athanasiou KA. Biphasic indentation of articular cartilage--II. A numerical algorithm and an experimental study. J Biomech. 1989; 22:853–861. [PubMed: 2613721]
27. Carrino DA, Arias JL, Caplan AI. A spectrophotometric modification of a sensitive densitometric Safranin O assay for glycosaminoglycans. Biochem Int. 1991; 24:485–495. [PubMed: 1772427]
28. Venn M, Maroudas A. Chemical composition and swelling of normal and osteoarthrotic femoral head cartilage. I. Chemical composition. Ann Rheum Dis. 1977; 36:121–129. [PubMed: 856064]
29. Fernandes RJ, Wilkin DJ, Weis MA, Wilcox WR, Cohn DH, Rimoin DL, Eyre DR. Incorporation of structurally defective type II collagen into cartilage matrix in kniest chondrodysplasia. Arch Biochem Biophys. 1998; 355:282–290. [PubMed: 9675039]
30. Fernandes RJ, Schmid TM, Eyre DR. Assembly of collagen types II, IX and XI into nascent hetero-fibrils by a rat chondrocyte cell line. Eur J Biochem. 2003; 270:3243–3250. [PubMed: 12869200]
31. Andreea SI, Marieta C, Anca D. AGEs and glucose levels modulate type I and III procollagen mRNA synthesis in dermal fibroblasts cells culture. Exp Diabetes Res. 2008; 2008:473603. [PubMed: 18401458]
32. Palamakumbura AH, Trackman PC. A fluorometric assay for detection of lysyl oxidase enzyme activity in biological samples. Anal Biochem. 2002; 300:245–251. [PubMed: 11779117]
33. Coral K, Angayarkanni N, Madhavan J, Bharathselvi M, Ramakrishnan S, Nandi K, Rishi P, Kasinathan N, Krishnakumar S. Lysyl oxidase activity in the ocular tissues and the role of LOX in proliferative diabetic retinopathy and rhegmatogenous retinal detachment. Invest Ophthalmol Vis Sci. 2008; 49:4746–4752. [PubMed: 18566459]
34. Fernandes RJ, Weis M, Scott MA, Seegmiller RE, Eyre DR. Collagen XI chain misassembly in cartilage of the chondrodysplasia (cho) mouse. Matrix Biol. 2007; 26:597–603. [PubMed: 17683922]
35. Fernandes RJ, Hirohata S, Engle JM, Colige A, Cohn DH, Eyre DR, Apte SS. Procollagen II amino propeptide processing by ADAMTS-3. Insights on dermatosparaxis. J Biol Chem. 2001; 276:31502–31509. [PubMed: 11408482]
36. McAlinden A, Traeger G, Hansen U, Weis MA, Ravindran S, Wirthlin L, Eyre DR, Fernandes RJ. Molecular properties and fibril ultrastructure of types II and XI collagens in cartilage of mice expressing exclusively the alpha1(IIA) collagen isoform. Matrix Biol. 2014; 34:105–113. [PubMed: 24113490]

37. Shoulders MD, Raines RT. Collagen structure and stability. Annu Rev Biochem. 2009; 78:929–958. [PubMed: 19344236]
38. Makris EA, MacBarb RF, Responte DJ, Hu JC, Athanasiou KA. A copper sulfate and hydroxylysine treatment regimen for enhancing collagen cross-linking and biomechanical properties in engineered neocartilage. FASEB J. 2013; 27:2421–2430. [PubMed: 23457219]
39. Asanbaeva A, Masuda K, Thonar EJ, Klisch SM, Sah RL. Cartilage growth and remodeling: modulation of balance between proteoglycan and collagen network in vitro with beta-aminopropionitrile. Osteoarthritis Cartilage. 2008; 16:1–11. [PubMed: 17631390]
40. Narayanan AS, Page RC, Kuzan F, Cooper CG. Elastin cross-linking in vitro. Studies on factors influencing the formation of desmosines by lysyl oxidase action on tropoelastin. Biochem J. 1978; 173:857–862. [PubMed: 30449]
41. Van Osch GJ, Mandl EW, Jahr H, Koevoet W, Nolst-Trenite G, Verhaar JA. Considerations on the use of ear chondrocytes as donor chondrocytes for cartilage tissue engineering. Biorheology. 2004; 41:411–421. [PubMed: 15299273]
42. Wathen P, Mitchell JW, Porter WP. Theoretical and experimental studies of energy exchange from jackrabbit ears and cylindrically shaped appendages. Biophys J. 1971; 11:1030–1047. [PubMed: 5134209]
43. Gilbert, SF. Developmental Biology. 6th. Sunderland (MA): Sinauer Associates; 2000. The Neural Crest.
44. Archer CW, Morrison H, Pitsillides AA. Cellular aspects of the development of diarthrodial joints and articular cartilage. J Anat. 1994; 184(Pt 3):447–456. [PubMed: 7928634]
45. Malda J, van Blitterswijk CA, van Geffen M, Martens DE, Tramper J, Riesle J. Low oxygen tension stimulates the redifferentiation of dedifferentiated adult human nasal chondrocytes. Osteoarthritis Cartilage. 2004; 12:306–313. [PubMed: 15023382]
46. Lohan A, Marzahn U, El Sayed K, Haisch A, Muller RD, Kohl B, Stolzel K, Ertel W, John T, Schulze-Tanzil G. Osteochondral articular defect repair using auricle-derived autologous chondrocytes in a rabbit model. Ann Anat. 2014; 196:317–326. [PubMed: 24812031]
47. Lohan A, Marzahn U, El Sayed K, Bock C, Haisch A, Kohl B, Stoelzel K, John T, Ertel W, Schulze-Tanzil G. Heterotopic and orthotopic autologous chondrocyte implantation using a minipig chondral defect model. Ann Anat. 2013; 195:488–497. [PubMed: 23742980]
48. Yokoyama A, Muneta T, Nimura A, Koga H, Mochizuki T, Hata Y, Sekiya I. FGF2 and dexamethasone increase the production of hyaluronan in two-dimensional culture of elastic cartilage-derived cells: in vitro analyses and in vivo cartilage formation. Cell Tissue Res. 2007; 329:469–478. [PubMed: 17587060]
49. Adam MF, Dorie MJ, Brown JM. Oxygen tension measurements of tumors growing in mice. Int J Radiat Oncol Biol Phys. 1999; 45:171–180. [PubMed: 10477021]
50. Gottrup F, Gellett S, Kirkegaard L, Hansen ES, Johannsen G. Continuous monitoring of tissue oxygen tension during hyperoxia and hypoxia: relation of subcutaneous, transcutaneous, and conjunctival oxygen tension to hemodynamic variables. Crit Care Med. 1988; 16:1229–1234. [PubMed: 3191740]
51. Brown W, Hill A. The oxygen-dissociation curve of blood, and its thermodynamical basis. Proceedings of the Royal Society of London. Series B, Containing Papers of a Biological Character. 1923:297–334.
52. Rappitsch G, Perktold K, Pernkopf E. Numerical modelling of shear-dependent mass transfer in large arteries. International Journal for Numerical Methods in Fluids. 1997; 25:847–857.
53. Stockwell, RA. Biology of cartilage cells. Cambridge: Cambridge University Press; 1979.
54. Coyle CH, Izzo NJ, Chu CR. Sustained hypoxia enhances chondrocyte matrix synthesis. J Orthop Res. 2009; 27:793–799. [PubMed: 19051248]
55. Domm C, Schunke M, Christesen K, Kurz B. Redifferentiation of dedifferentiated bovine articular chondrocytes in alginate culture under low oxygen tension. Osteoarthritis Cartilage. 2002; 10:13–22. [PubMed: 11795979]
56. Egli RJ, Bastian JD, Ganz R, Hofstetter W, Leunig M. Hypoxic expansion promotes the chondrogenic potential of articular chondrocytes. J Orthop Res. 2008; 26:977–985. [PubMed: 18302236]

57. Hansen U, Schunke M, Domm C, Ioannidis N, Hassenpflug J, Gehrke T, Kurz B. Combination of reduced oxygen tension and intermittent hydrostatic pressure: a useful tool in articular cartilage tissue engineering. J Biomech. 2001; 34:941–949. [PubMed: 11410177]
58. Makris EA, Hu JC, Athanasiou KA. Hypoxia-induced collagen crosslinking as a mechanism for enhancing mechanical properties of engineered articular cartilage. Osteoarthritis Cartilage. 2013; 21:634–641. [PubMed: 23353112]
59. Meretoja VV, Dahlin RL, Wright S, Kasper FK, Mikos AG. The effect of hypoxia on the chondrogenic differentiation of co-cultured articular chondrocytes and mesenchymal stem cells in scaffolds. Biomaterials. 2013; 34:4266–4273. [PubMed: 23489925]
60. Yodmuang S, Gadjanski I, Chao PH, Vunjak-Novakovic G. Transient hypoxia improves matrix properties in tissue engineered cartilage. J Orthop Res. 2013; 31:544–553. [PubMed: 23203946]
61. Ysart GE, Mason RM. Responses of articular cartilage explant cultures to different oxygen tensions. Biochim Biophys Acta. 1994; 1221:15–20. [PubMed: 8130272]
62. Qu C, Lindeberg H, Ylarinne JH, Lammi MJ. Five percent oxygen tension is not beneficial for neocartilage formation in scaffold-free cell cultures. Cell Tissue Res. 2012; 348:109–117. [PubMed: 22392735]
63. Pawelek JM. Effects of thyroxine and low oxygen tension on chondrogenic expression in cell culture. Dev Biol. 1969; 19:52–72. [PubMed: 5767095]
64. Babur BK, Ghanavi P, Levett P, Lott WB, Klein T, Cooper-White JJ, Crawford R, Doran MR. The interplay between chondrocyte redifferentiation pellet size and oxygen concentration. PLoS One. 2013; 8:e58865. [PubMed: 23554943]
65. Collins JA, Moots RJ, Winstanley R, Clegg PD, Milner PI. Oxygen and pH-sensitivity of human osteoarthritic chondrocytes in 3-D alginate bead culture system. Osteoarthritis Cartilage. 2013; 21:1790–1798. [PubMed: 23850530]
66. Dare EV, Griffith M, Poitras P, Wang T, Dervin GF, Giulivi A, Hincke MT. Fibrin sealants from fresh or fresh/frozen plasma as scaffolds for in vitro articular cartilage regeneration. Tissue Eng Part A. 2009; 15:2285–2297. [PubMed: 19226200]
67. Das RH, van Osch GJ, Kreukniet M, Oostra J, Weinans H, Jahr H. Effects of individual control of pH and hypoxia in chondrocyte culture. J Orthop Res. 2010; 28:537–545. [PubMed: 19813243]
68. Duval E, Leclercq S, Elissalde JM, Demoor M, Galera P, Boumediene K. Hypoxia-inducible factor 1alpha inhibits the fibroblast-like markers type I and type III collagen during hypoxia-induced chondrocyte redifferentiation: hypoxia not only induces type II collagen and aggrecan, but it also inhibits type I and type III collagen in the hypoxia-inducible factor 1alpha-dependent redifferentiation of chondrocytes. Arthritis Rheum. 2009; 60:3038–3048. [PubMed: 19790048]
69. Duval E, Bauge C, Andriamanalijaona R, Benateau H, Leclercq S, Dutoit S, Poulain L, Galera P, Boumediene K. Molecular mechanism of hypoxia-induced chondrogenesis and its application in in vivo cartilage tissue engineering. Biomaterials. 2012; 33:6042–6051. [PubMed: 22677190]
70. Koay EJ, Athanasiou KA. Hypoxic chondrogenic differentiation of human embryonic stem cells enhances cartilage protein synthesis and biomechanical functionality. Osteoarthritis Cartilage. 2008; 16:1450–1456. [PubMed: 18541445]
71. Foldager CB, Nielsen AB, Munir S, Ulrich-Vinther M, Soballe K, Bunger C, Lind M. Combined 3D and hypoxic culture improves cartilage-specific gene expression in human chondrocytes. Acta Orthop. 2011; 82:234–240. [PubMed: 21434761]
72. Gawlitta D, van Rijen MH, Schrijver EJ, Alblas J, Dhert WJ. Hypoxia impedes hypertrophic chondrogenesis of human multipotent stromal cells. Tissue Eng Part A. 2012; 18:1957–1966. [PubMed: 22563686]
73. Murphy CL, Polak JM. Control of human articular chondrocyte differentiation by reduced oxygen tension. J Cell Physiol. 2004; 199:451–459. [PubMed: 15095292]
74. Schrobback K, Klein TJ, Crawford R, Upton Z, Malda J, Leavesley DI. Effects of oxygen and culture system on in vitro propagation and redifferentiation of osteoarthritic human articular chondrocytes. Cell Tissue Res. 2012; 347:649–663. [PubMed: 21638206]
75. Strobel S, Loparic M, Wendt D, Schenk AD, Candrian C, Lindberg RL, Moldovan F, Barbero A, Martin I. Anabolic and catabolic responses of human articular chondrocytes to varying oxygen percentages. Arthritis Res Ther. 2010; 12:R34. [PubMed: 20193091]

76. Thoms BL, Murphy CL. Inhibition of hypoxia-inducible factor-targeting prolyl hydroxylase domain-containing protein 2 (PHD2) enhances matrix synthesis by human chondrocytes. J Biol Chem. 2010; 285:20472–20480. [PubMed: 20404338]

77. Thoms BL, Dudek KA, Lafont JE, Murphy CL. Hypoxia promotes the production and inhibits the destruction of human articular cartilage. Arthritis Rheum. 2013; 65:1302–1312. [PubMed: 23334958]

78. Legendre F, Ollitrault D, Hervieu M, Bauge C, Maneix L, Goux D, Chajra H, Mallein-Gerin F, Boumediene K, Galera P, Demoor M. Enhanced hyaline cartilage matrix synthesis in collagen sponge scaffolds by using siRNA to stabilize chondrocytes phenotype cultured with bone morphogenetic protein-2 under hypoxia. Tissue Eng Part C Methods. 2013; 19:550–567. [PubMed: 23270543]

79. Brighton CT, Lane JM, Koh JK. In vitro rabbit articular cartilage organ model. II. 35S incorporation in various oxygen tensions. Arthritis Rheum. 1974; 17:245–252. [PubMed: 4274942]

80. Buckley CT, Vinardell T, Kelly DJ. Oxygen tension differentially regulates the functional properties of cartilaginous tissues engineered from infrapatellar fat pad derived MSCs and articular chondrocytes. Osteoarthritis Cartilage. 2010; 18:1345–1354. [PubMed: 20650328]

81. Fermor B, Christensen SE, Youn I, Cernanec JM, Davies CM, Weinberg JB. Oxygen, nitric oxide and articular cartilage. Eur Cell Mater. 2007; 13:56–65. discussion 65. [PubMed: 17427142]

82. Meyer EG, Buckley CT, Thorpe SD, Kelly DJ. Low oxygen tension is a more potent promoter of chondrogenic differentiation than dynamic compression. J Biomech. 2010; 43:2516–2523. [PubMed: 20557888]

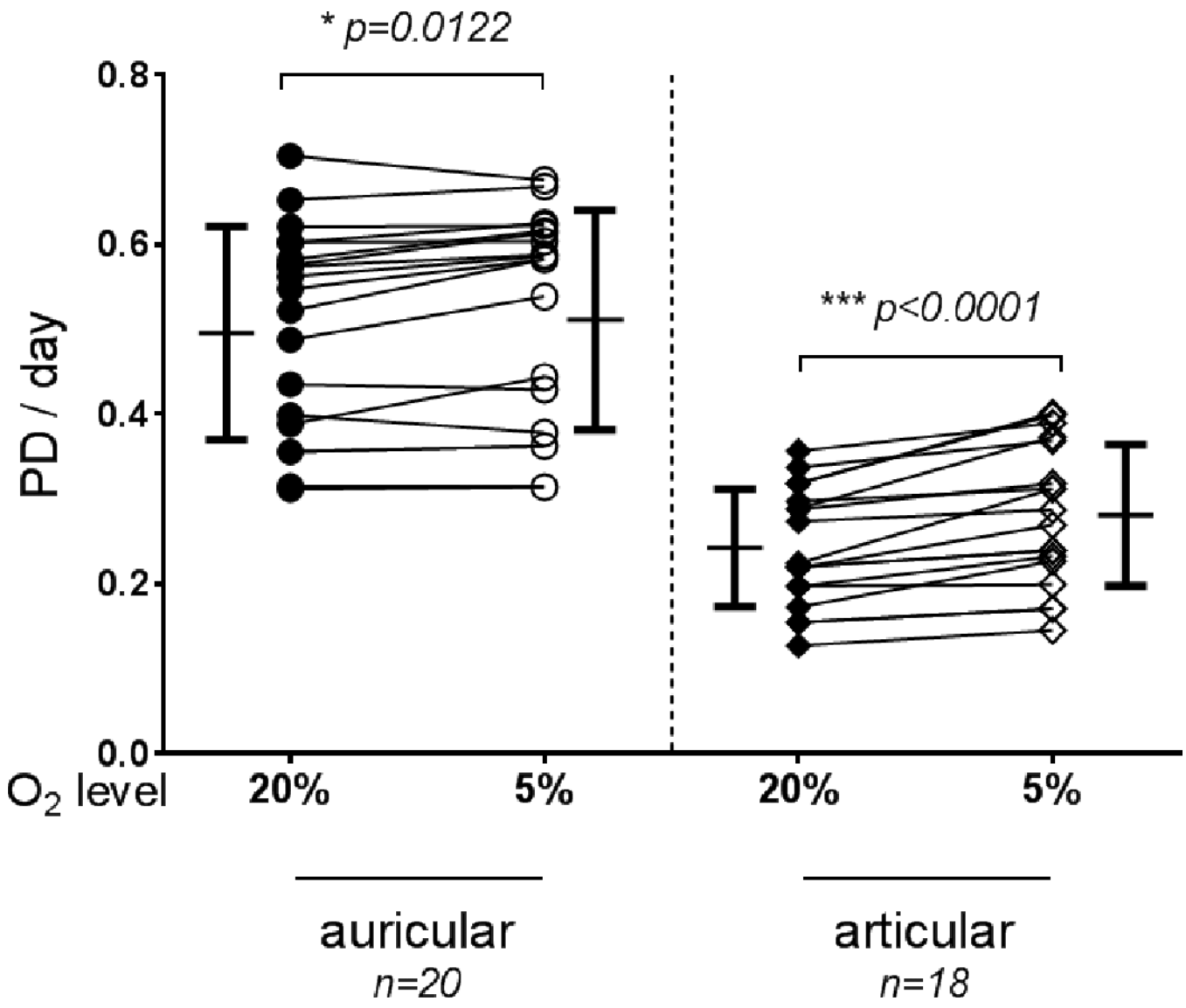

Figure 1.

Comparison of proliferation rates under different oxygen tensions. Low oxygen tension increased the rate of proliferation for both auricular and articular chondrocytes. This increase was greater for articular chondrocytes (16% vs. 3%). Auricular chondrocytes proliferated 2-fold faster than articular chondrocytes at 20% O_2 and 1.8-fold faster at 5% O_2 ($p < 0.0001$). Symbols indicate the mean for an experiment, and lines connect experiments. Bars show mean ± S.D.

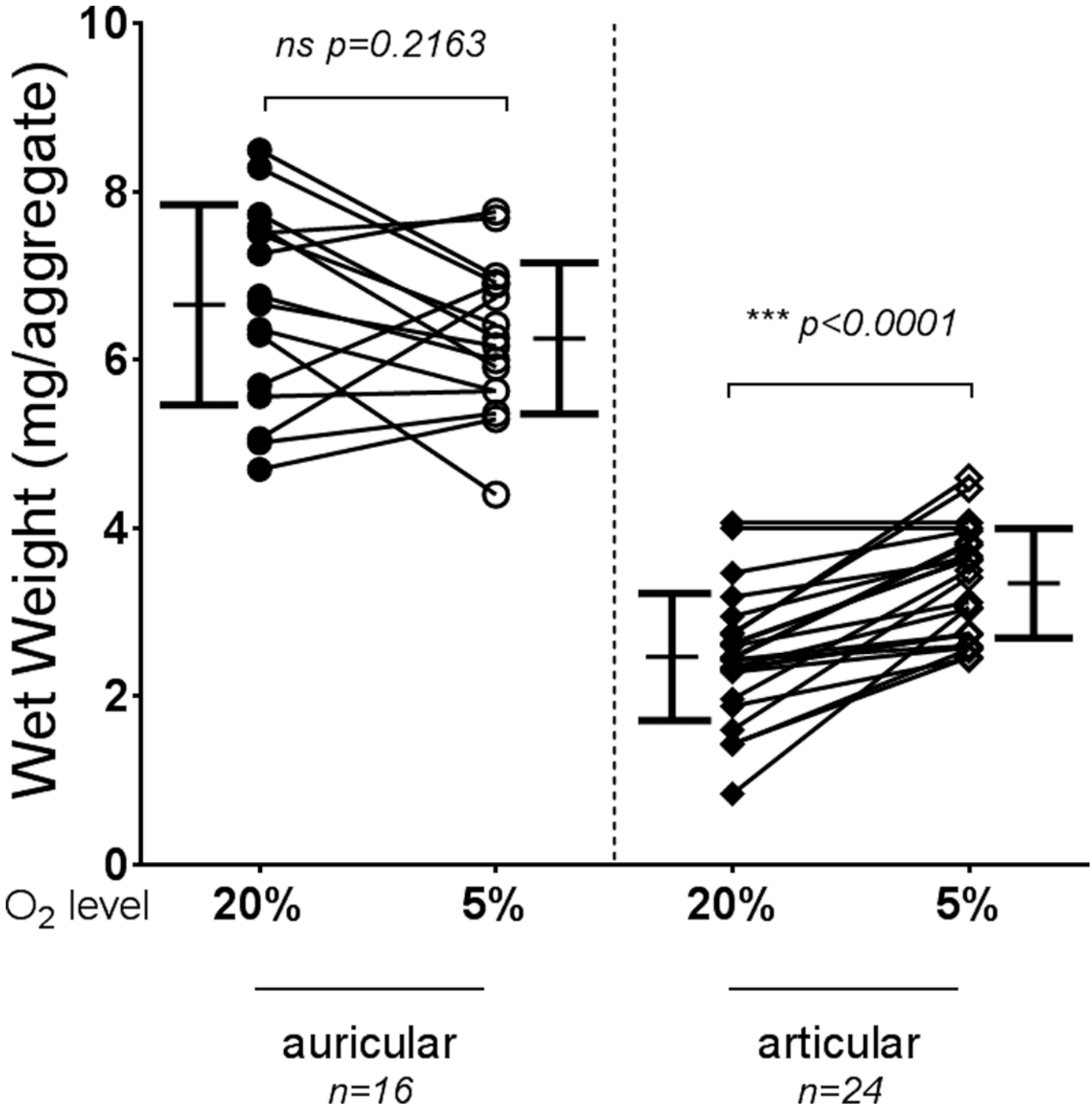

Figure 2.

Aggregate wet weights from chondrocytes grown and differentiated at 5% and 20% O_2. Wet weight was not significantly different between aggregates cultured at either oxygen tension for auricular chondrocytes but was significantly enhanced by low oxygen tension for articular chondrocytes. Auricular chondrocytes produce aggregates that are significantly heavier regardless of oxygen tension ($p < 0.0001$). Symbols indicate the mean for an experiment, and lines connect experiments. Bars show mean ± S.D.

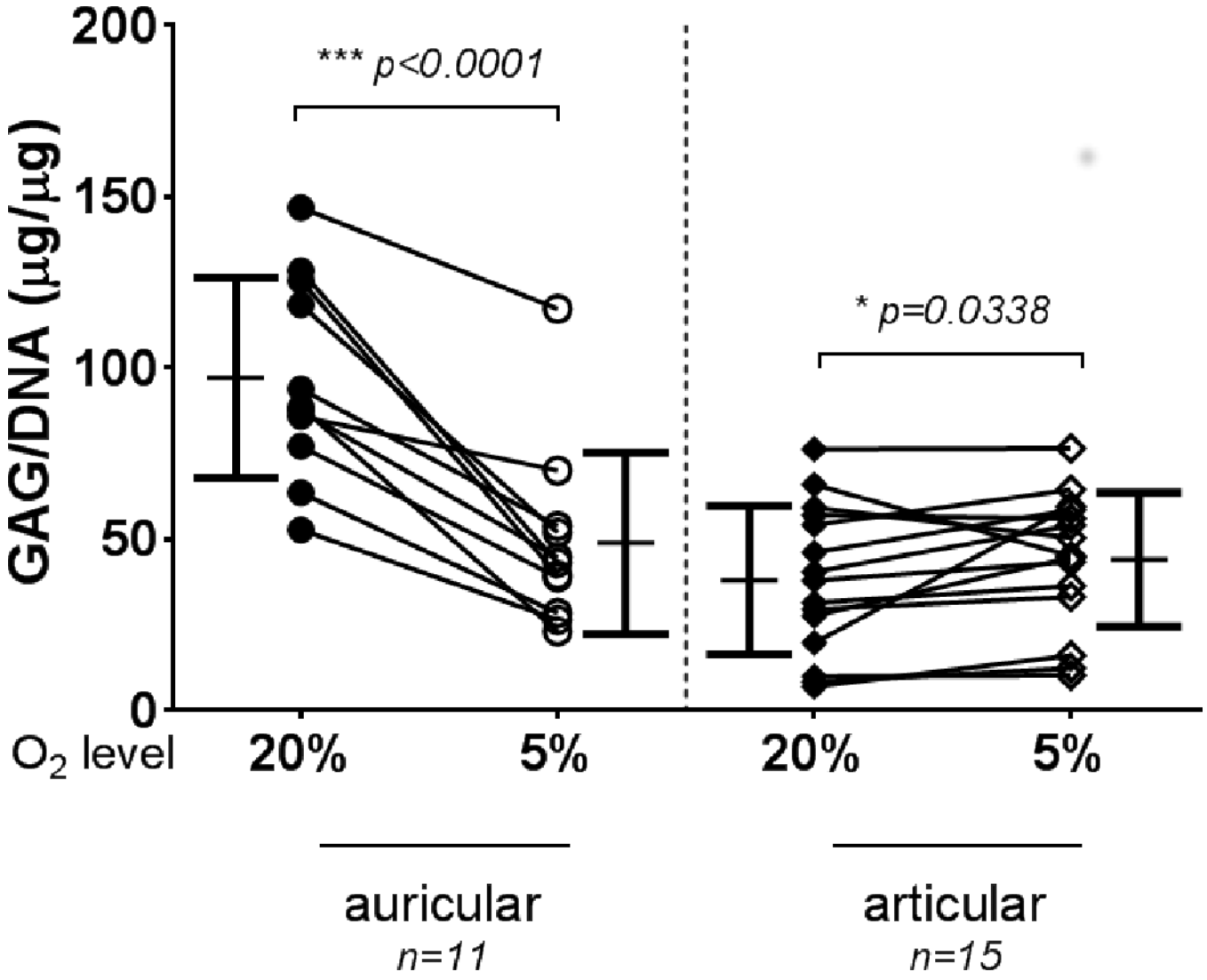

Figure 3.

GAG accumulation in aggregates. Auricular chondrocyte aggregates cultured under low oxygen tension accumulated significantly less GAG than those cultured at standard O_2. Articular chondrocytes displayed the opposite trend and accumulated significantly more GAG at low O_2. Auricular chondrocyte aggregates grown at standard O_2 had significantly more GAG than articular chondrocyte aggregates ($p < 0.0001$). Symbols indicate the mean of an experiment, and lines connect the experiment. Bars show mean ± S.D.

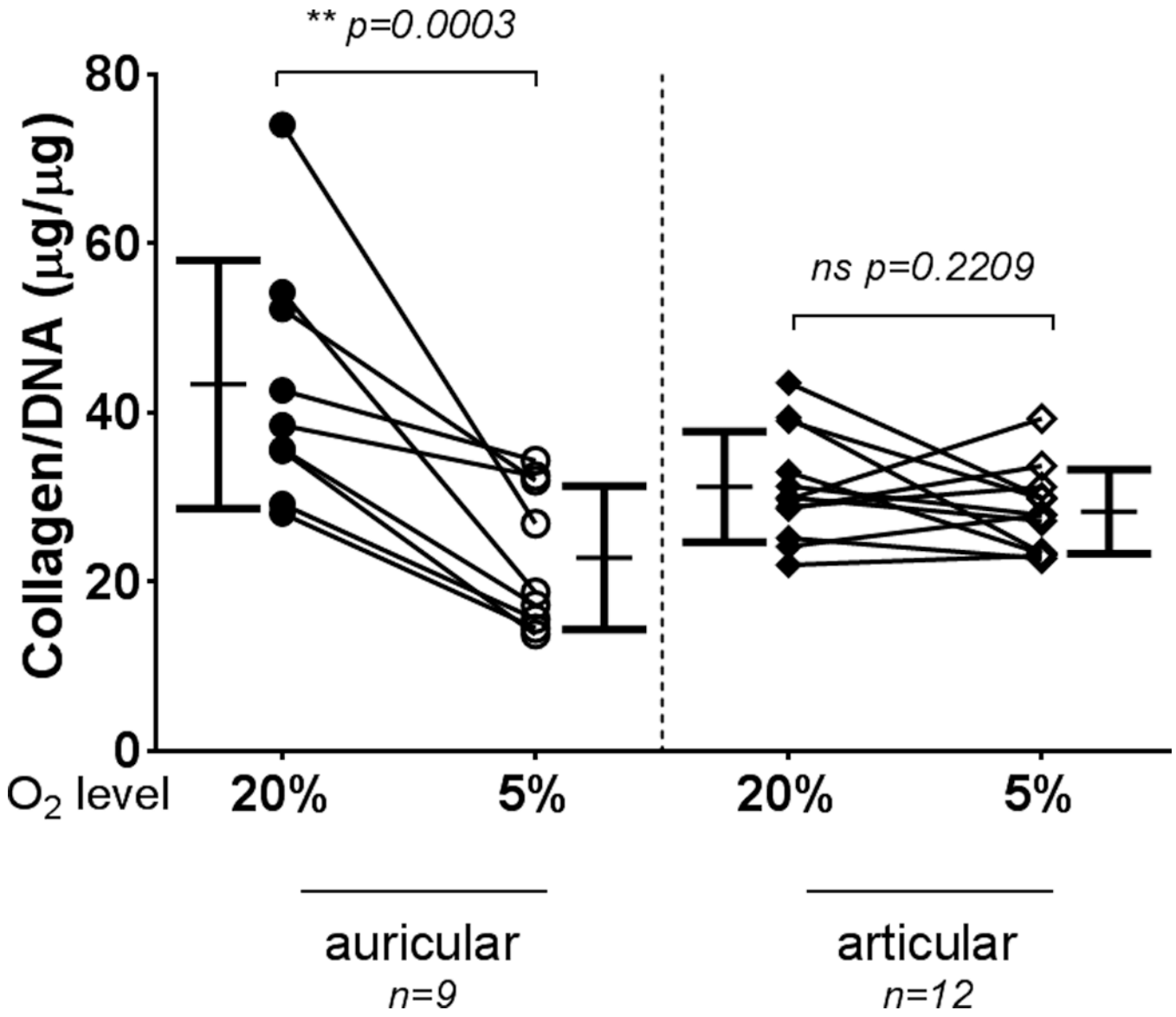

Figure 4.

Collagen accumulation in aggregates. Auricular chondrocyte aggregates cultured under low oxygen tension had significantly less collagen content than those cultured at standard O_2. No consistent effect on collagen content was evident for articular chondrocytes. Symbols indicate the mean from an experiment, and lines connect the experiment. Bars show mean ± S.D.

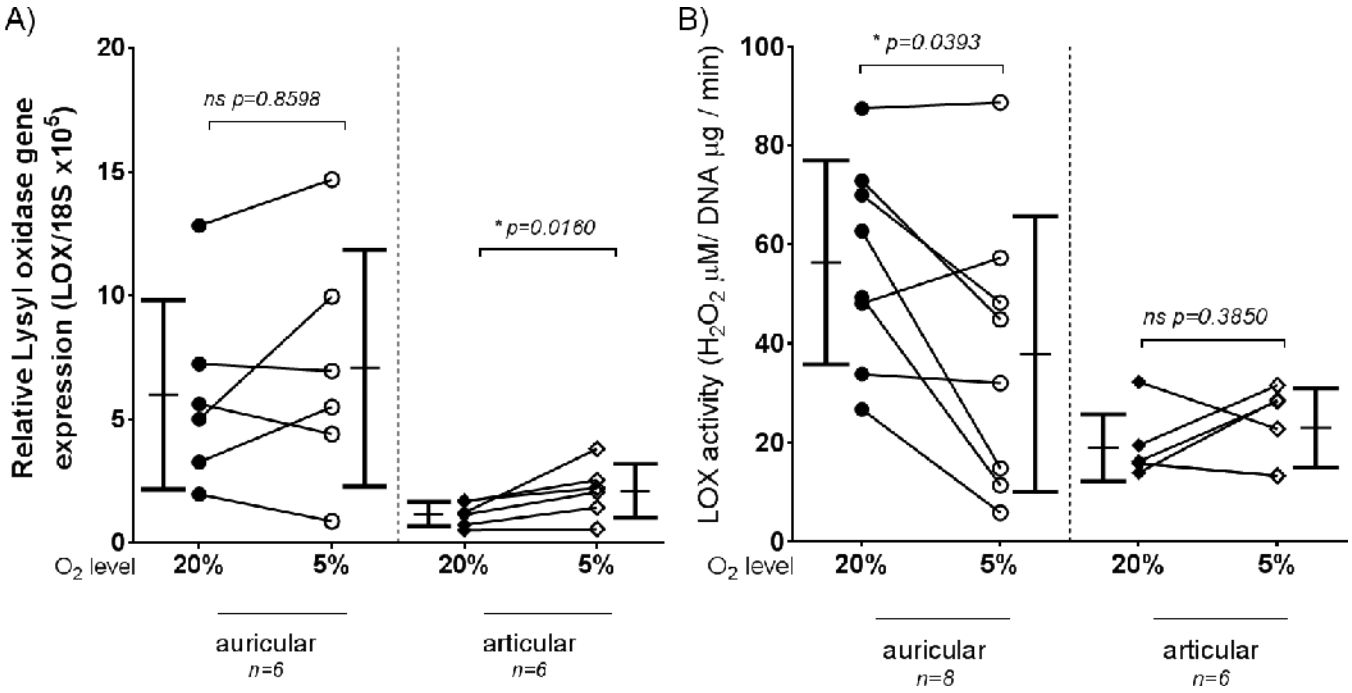

Figure 5.

Lysyl oxidase expression and activity in aggregates. (A) Oxygen tension had no consistent effect on lysyl oxidase expression in auricular chondrocyte aggregates. LOX trended toward higher expression at low oxygen tension with articular chondrocyte aggregates. Auricular chondrocytes had significantly higher gene expression than articular chondrocytes of lysyl oxidase at each oxygen tension ($p < 0.05$). (B) In terms of activity, there was a significant decrease in auricular chondrocytes grown under low oxygen tension but no significant effect on the articular chondrocytes. Lysyl oxidase activity was significantly higher per cell in auricular chondrocytes over articular chondrocytes only at 20% oxygen tension ($p < 0.05$). Symbols indicate the mean from an experiment, and lines connect the experiment. Bars show mean ± S.D.

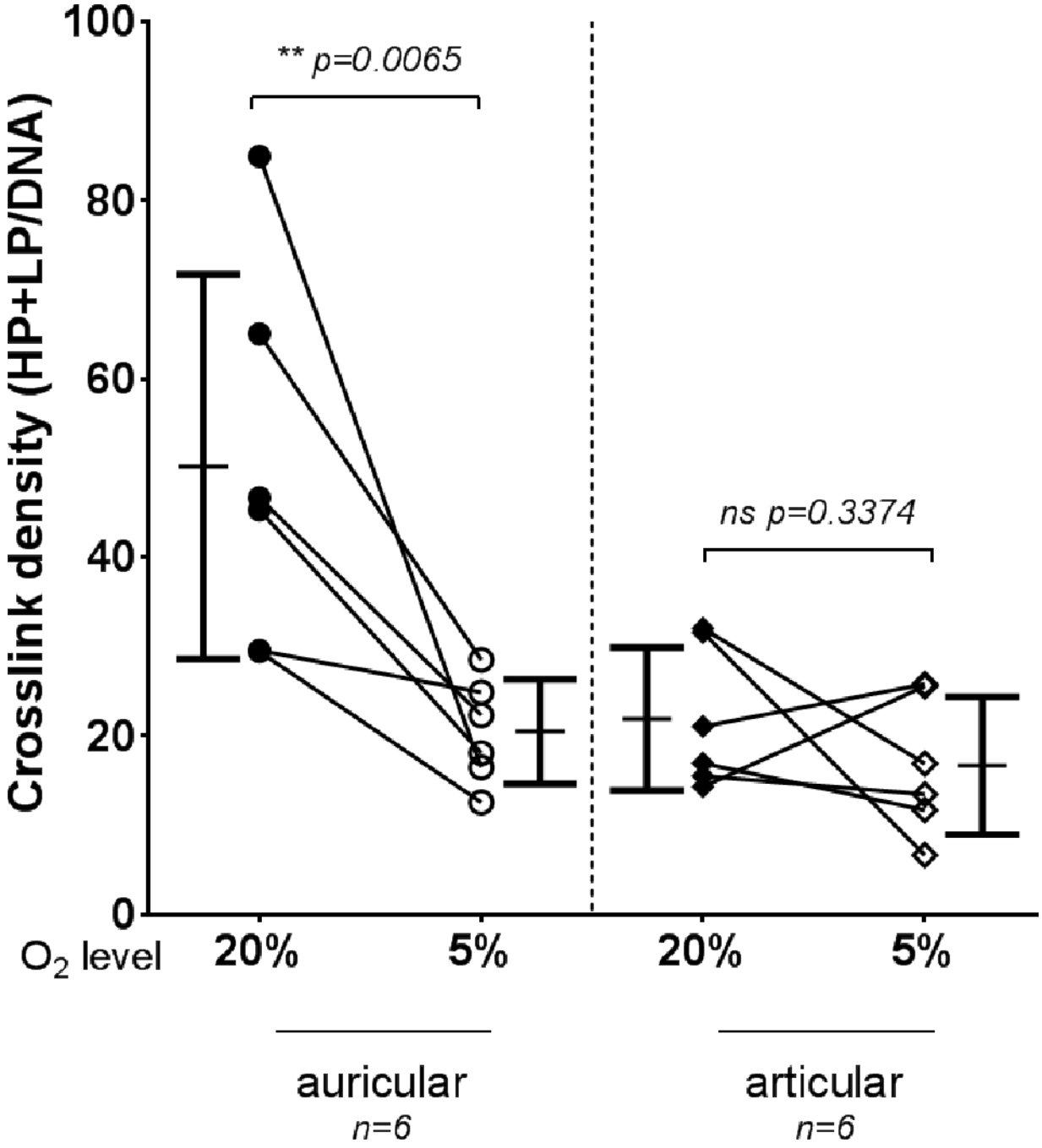

Figure 6.

Collagen cross-link density in aggregates. Collagen cross-link density was significantly lower for auricular chondrocyte tissue grown at low oxygen tension, but no consistent change was seen for the articular chondrocytes. Auricular chondrocytes grown at standard O_2 had significantly more cross-linking ($p < 0.01$). Symbols indicate the mean from an experiment, and lines connect the experiment. Bars show mean ± S.D.

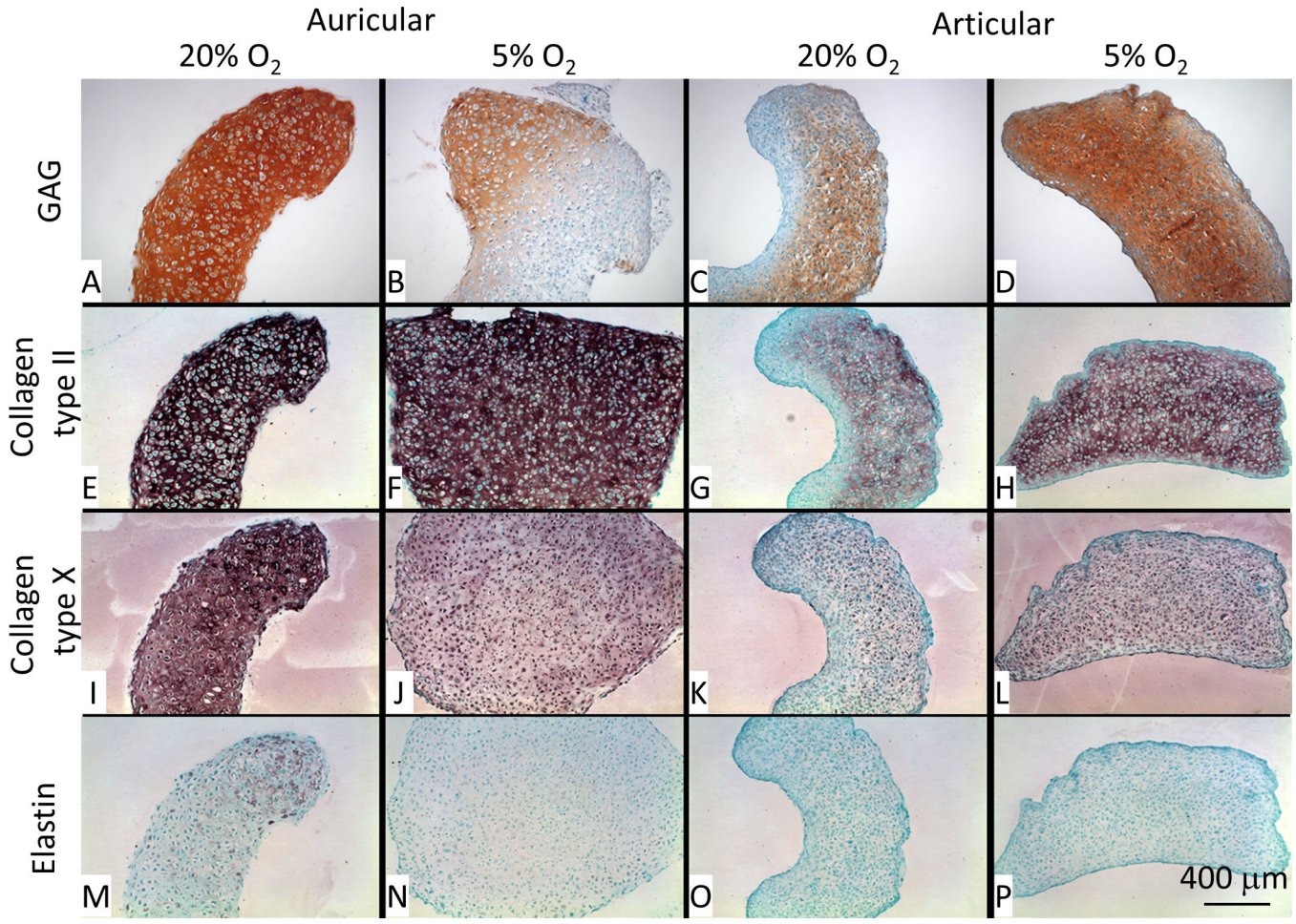

Figure 7.

Histology and immunohistochemistry. Safranin-O/Fast green staining shows greater accumulation of GAG in auricular chondrocyte aggregates differentiated at 20% O_2 vs. 5% O_2; the reverse is true for the articular cartilage aggregates. Collagen type II staining (E–H) shows no apparent difference in the auricular chondrocyte aggregates but is clearly stronger in articular chondrocyte aggregates at 5% O_2 vs. 20% O_2. Collagen type X staining (I–L) is stronger in auricular chondrocyte aggregates at 20% O_2 vs. 5% O_2 and is more matrix associated. In articular chondrocyte aggregates, there is a slightly stronger staining at 5% O_2 vs. 20% O_2. Elastin staining (M–P) was weak across all samples with a slightly greater accumulation at 20% O_2 for the auricular chondrocyte aggregates only.

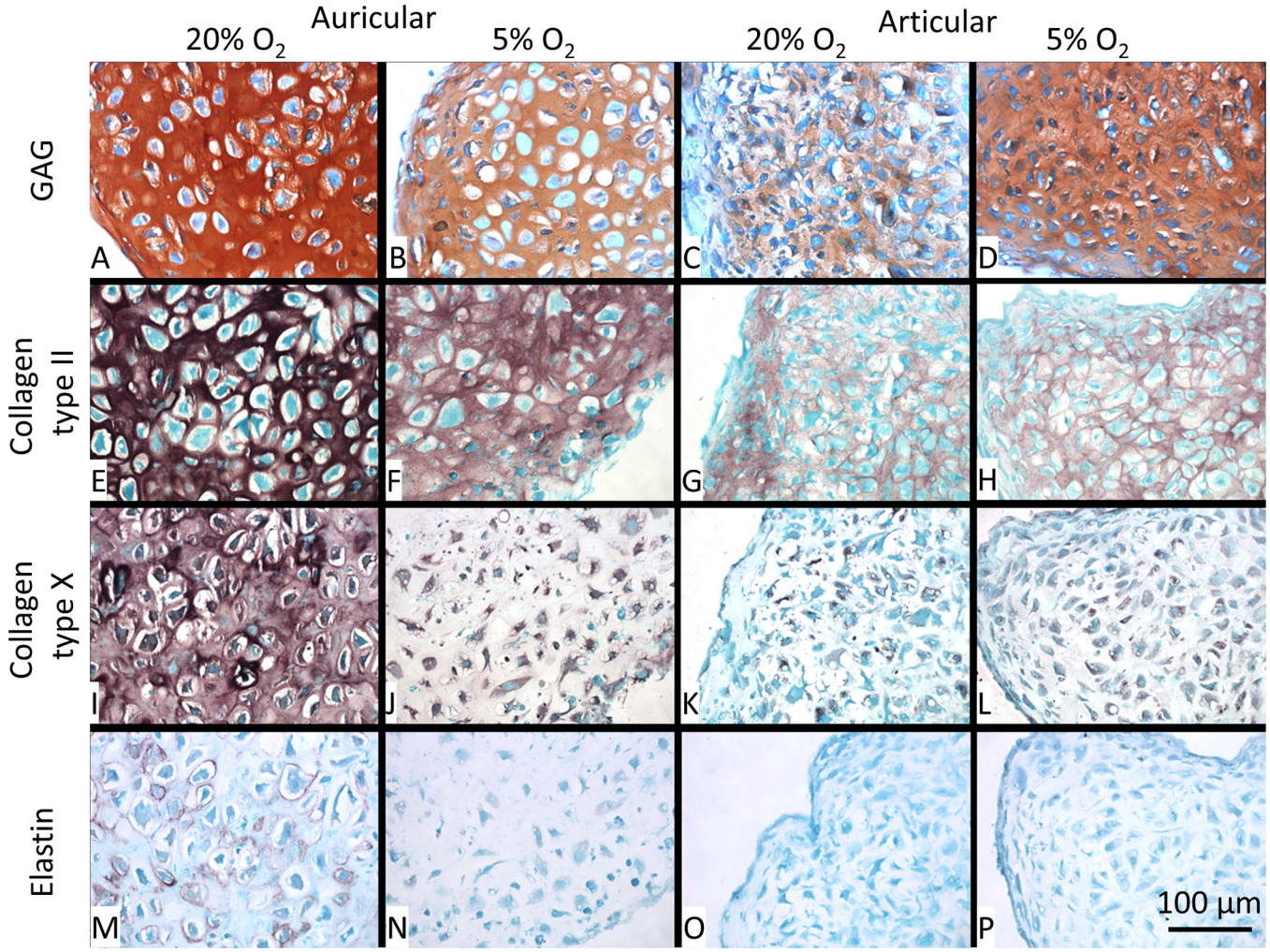

Figure 8.

Higher magnification histology and immunohistochemistry. Safranin-O/Fast green staining shows greater accumulation of GAG in auricular chondrocyte aggregates differentiated at 20% O_2 vs. 5% O_2; the reverse is true for the articular cartilage aggregates (A–D). Collagen type II staining (E–H) shows no apparent difference in the auricular chondrocyte aggregates but is clearly stronger in articular chondrocyte aggregates at 5% O_2 vs. 20% O_2. Collagen type X staining (I–J) is stronger in auricular chondrocyte aggregates at 20% O_2 vs. 5% O_2 and is more matrix associated. In articular chondrocyte aggregates there is a slightly stronger staining at 5% O_2 vs. 20% O_2. Elastin staining (M–P) was weak across all samples with a greater accumulation at 20% O_2 for the auricular chondrocyte aggregates only.

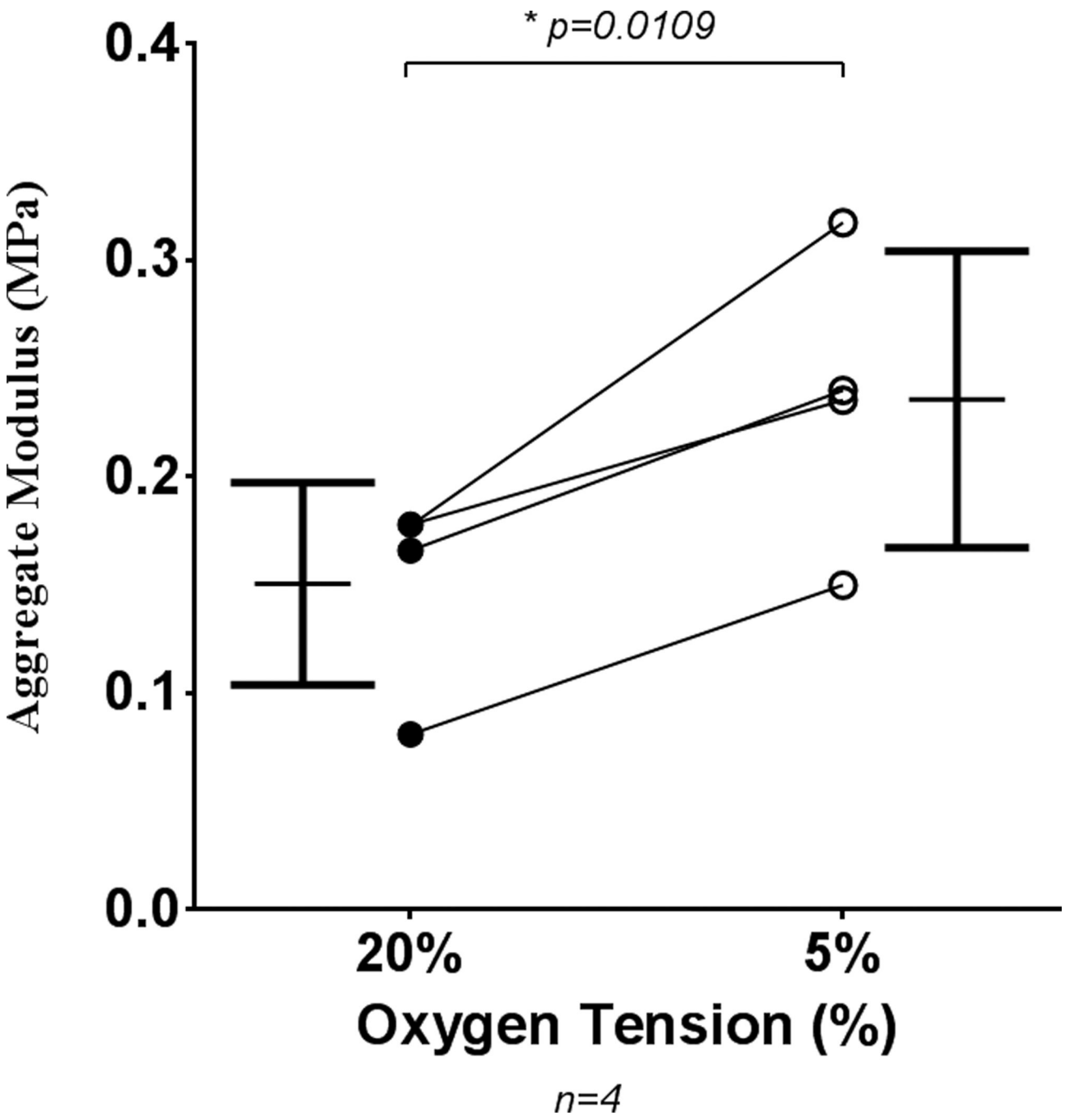

Figure 9.

Biomechanical testing of articular chondrocyte sheets. Articular chondrocyte derived, scaffold-free, tissue engineered sheets have greater mechanical stiffness when cultured at low (5%) oxygen tension than at standard (20%) O_2. Auricular sheets did not form testable constructs at low oxygen tension. Symbols indicate the mean from an experiment, and lines connect the experiment. Bars show mean ± S.D.

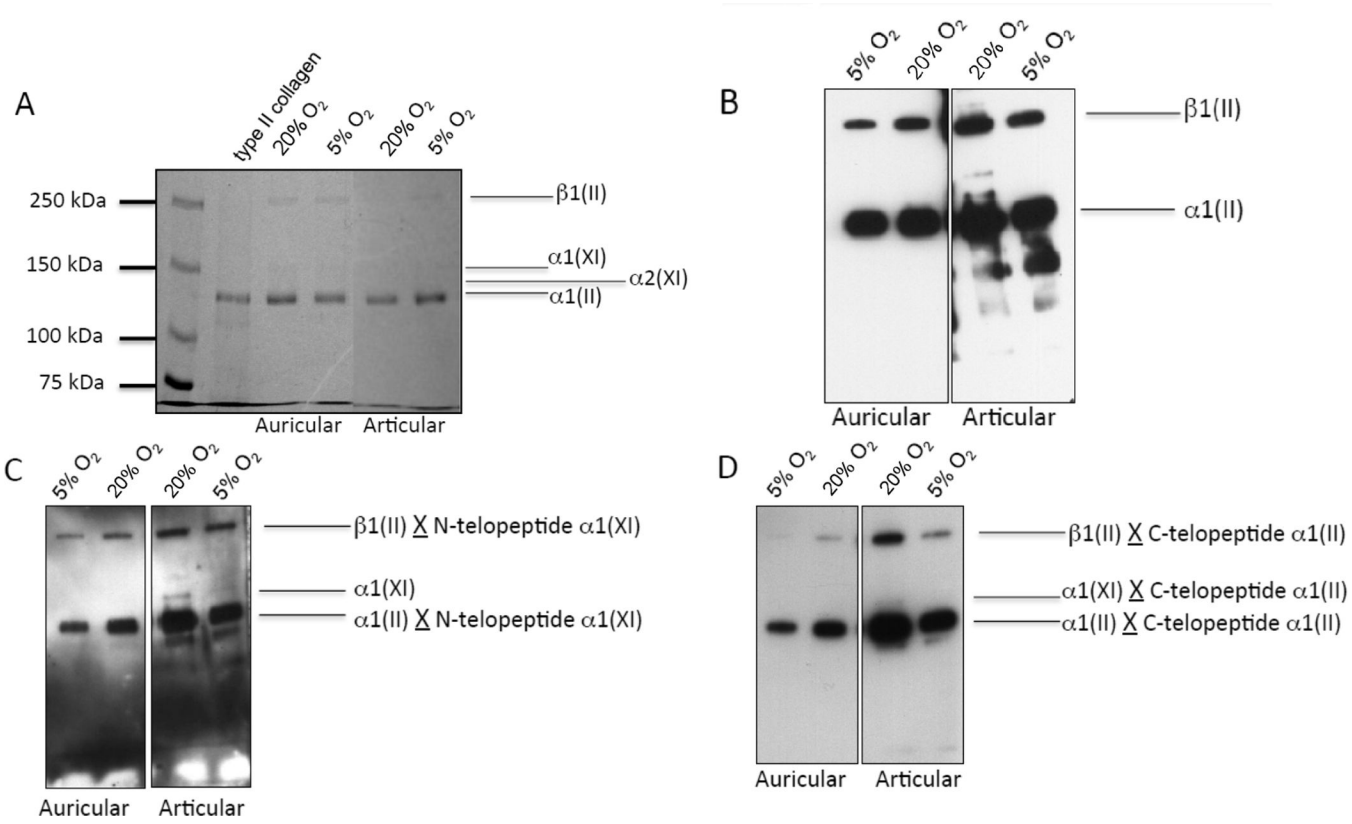

Figure 10.

Type II and type XI collagen heterpolymer formation in aggregates. (A) Coomasie blue-stained SDS-PAGE gel of pepsin solubilized collagen showing α1(II), α1(XI), α2(XI) and α1(II) chains. (B) Western blot of samples equivalent to those in A and probed with anti-type II collagen antibody (1C10) confirmed type II collagen chains synthesized by auricular and articular chondrocytes under standard and low O_2 conditions. (C) Western blot of samples identical to those in B and probed with antibody 5890. This antibody specifically recognizes the N-telopeptide domain of α1(XI) collagen when cross- linked to chains of α1(II) and β1(II). (D) Western blot of samples identical to those electrophoresed in B (above) and probed with mAb 10F2. This antibody specifically recognizes the C- telopeptide domain of type II collagen when it is cross-linked to α1(II) collagen chains as we have shown before for murine cartilage (34). The antibody also detected the α1(XI) chain in articular chondrocyte matrix grown in 20% O_2 but not under 5% O_2.

Table 1

Effect of reduced oxygen tension on *in vitro* chondrogenesis

Species	Cells	Differentiation Format	GAG	Collagen	Mechanical testing	Gene	Harvest time	Expansion Passages and O_2	Differentiation O_2	Reference
Bo	ACs	Alginate beads	+	+	N/A	+	d1, d3, d10, d17	None	2, 21%	(54)
Bo	ACs	Alginate beads	+	+	N/A	N/A	2 wk, 3 wk	P1 5, 21%	5, 21%	(55)
Bo	ACs	Pellet	−	=	N/A	+/−	d14	P1 1.5, 21%	1.5, 5, 21%	(56)
Bo	ACs	Alginate beads	N/A	N/A	N/A	=	d2, d7	None	0.1, 5, 10, 20%	(19)
Bo	ACs	Monolayer	N/A	+	N/A	N/A	d4	None	5, 21%	(57)
Bo	ACs	5mm diameter disc in agarose	=	−	=		d28	P1 21%	4, 21%	(58)
Bo	ACs, MSCs	Electrospun PCL	+	−	N/A	+	d0, d14, d28, d42	P1-2 21%	5, 20%	(59)
Bo	ACs	Agarose	−	−	−	−	d7, d14, d21, d28	None	5, 21%	(60)
Bo	ACs	Explant	−	N/A	N/A	N/A	d0, d1, d5, d7	None	6, 10, 24, 66, 91%	(61)
Bo	ACs	Self assembling	−	−	N/A	−	2wk, 4wk, 6wk	None	5, 20%	(62)
Ga	SCs	Monolayer	+	N/A	N/A	N/A	2wk, 4wk	None	5, 21%	(63)
Hu	ACs	Pellet	+	=	N/A	N/A	d21	P2-4, 5&20%	5, 20%	(6)
Hu	ACs	Micropellets	+	+	N/A	+	d4, d7, d11, d14	P3 2%	2, 20%	(64)
Hu	ACs	Alginate beads	+	N/A	N/A	N/A	d1, d2, d4	P3 5%	<1, 2, 5, 21%	(65)
Hu	ACs	fibrin glue, genipincross-linked	+	−	=	+	d1, 2.5wk, 7wk	P0 21%	5, 21%	(66)
Hu	ACs	Alginate beads	N/A	N/A	N/A	+	d5	P3 21%	5, 20%	(67)
Hu	ACs	Alginate beads	=	=	N/A	+	d21	P2-3 21%	5, 21%	(68)
Hu	MSCs	Alginate beads	+	=	N/A	+/−	d21	P5 21%	5, 21%	(69)
Hu	ACs	Alginate beads	+	=	N/A	+/−	d21	P2 21%	5, 21%	(69)
Hu	ESCs	Self assembling	−	+	+	N/A	4wk	1P* 2, 20%	2, 20%	(70)
Hu	NCs	Pellet	+	=	N/A	N/A	d21	P2 21%	1, 5.25, 21%	(45)
Hu	ACs	MPEG-PLGA	N/A	N/A	N/A	+	d1, d2, d6	P2 21%	1, 5, 21%	(71)
Hu	BM MSCs	Pellet	+/−	+/−	N/A	+/−	4wk	P2-4 21%	5, 20%	(72)
Hu	ACs	Alginate beads	+	N/A	N/A	+	d7,d14,d28	P3 20%	5, 20%	(73)
Hu	ACs	Pellet	+	+	N/A	+	d7, d14, d28	P3 5, 20%	5, 20%	(74)
Hu	ACs	Pellet	+	+	N/A	+	2wk, 4wk	P2 5, 19%	5, 19%	(75)

Species	Cells	Differentiation Format	GAG	Collagen	Mechanical testing	Gene	Harvest time	Expansion Passages and O_2	Differentiation O_2	Reference
Hu	ACs	Monolayer	N/A	+	N/A	+	d3	P0-3 20%	1, 20%	(76)
Hu, Sus, Mu	AC explants	Explants	N/A	N/A	N/A	+	d3	P0-3 20%	1, 20%	(77)
Hu, Rb	ACs	Type I and III collagen sponge	+	+	N/A	+	d0, d3, d7, d14	P1 21%	3, 21%	(78)
Rb	Articular slices	Explant	−	N/A	N/A	N/A	d7	None	1, 5, 21, 35, 60, 90%	(79)
Rb	ACs	Pellet	+	+	N/A	+	d3, d7, d21	P1 5, 21%	5, 21%	(12)
Sus	ACs	Agarose	+	=	−	N/A	d21, d42	P1 20%	5, 20%	(80)
Sus	Fat pad MSCs	Agarose	+	=	+	N/A	d21, d42	P3 20%	5, 20%	(80)
Sus	AC explants	Explant	N/A	N/A	+	N/A	d6	None	5, 21%	(81)
Sus	BM MSCs	Agarose	+	=	+	N/A	d21, d42	P3 21%	5, 21%	(82)

Green indicates positive results, red indicates negative results and orange indicates no effect on chondrogenesis due to oxygen tension.

Hu = Human, Bo = Bovine, Ga = Chicken, Sus = Porcine, Mu = Murine; ACs = Articular Chondrocytes, MSCs = Mesenchymal Stem Cells, ESCs = Embryonic Stem Cells, NCs = Nasal Chondrocytes, SCs = Sternal Chondrocytes;* p38 human ESCs used, 1 passage (P) thereafter.